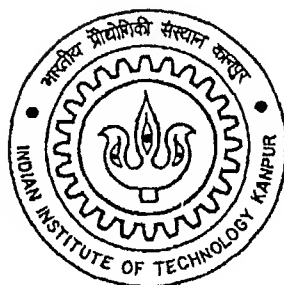


# Order Reduction and Vibration Minimisation in Helicopter Fuselage

by  
Anita Mathews

TH  
EE/1998/M  
M4220



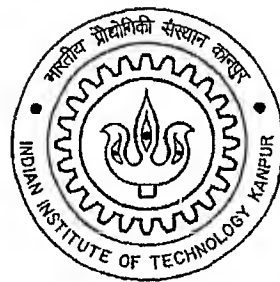
DEPARTMENT OF ELECTRICAL ENGINEERING  
INDIAN INSTITUTE OF TECHNOLOGY KANPUR

October, 1998

# **Order Reduction and Vibration Minimisation in Helicopter Fuselage**

by

Anita Mathews



DEPARTMENT OF ELECTRICAL ENGINEERING  
**INDIAN INSTITUTE OF TECHNOLOGY KANPUR**

October, 1998

# Order Reduction and Vibration Minimisation in Helicopter Fuselage

*A Thesis Submitted*  
*in Partial Fulfillment of the Requirements*  
*for the Degree of*  
*Master of Technology*

*by*

*Anita Mathews*



*to the*

DEPARTMENT OF  
ELECTRICAL ENGINEERING  
INDIAN INSTITUTE OF TECHNOLOGY, KANPUR

*October 1998*

4 JUN 1999 /EE

CENTRAL LIBRARY  
I. I. T. KANPUR

Iss. No. A

~~126846~~

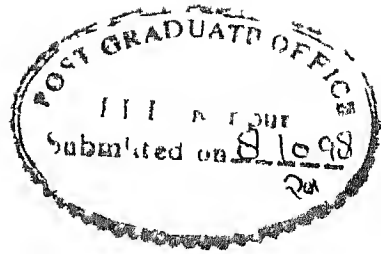
126846

-1 H  
EE/1998-1-1  
M11 C

EE-1998-M- Mat - ord



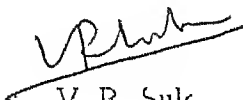
A126846



## CERTIFICATE

This is to certify that the work contained in the thesis entitled Order Reduction And Vibration Minimisation in Helicopter Fuselage by Anita Mathews, has been carried out under our supervision and that this work has not been submitted elsewhere for a degree

2

  
V R Sule

Deptt of Electrical Engineering

  
C Venkatesan

Deptt of Aerospace Engineering

Indian Institute of Technology,

Kharagpur

Date 8/10/98

## **Abstract**

The reduction of helicopter vibration remains a major challenge to the rotorcraft designer. The present study addresses the problem of formulation and design of a multi-input-multi output closed loop vibration control scheme, of a 3 D flexible fuselage model based on the concept of ACSR(Active Control Of Structural Response). The sensor locations for vibration measurement are chosen from a optimal set of locations measuring high levels of vibration. Initially the dynamic model of the full order system is decomposed into flexible and rigid body mode subsystems. A reduced order model for the flexible mode system is formulated using balanced realisation based-order reduction technique. Controller is then designed for this reduced model using factorisation theory and internal model principle for disturbance rejection. The simulation study showed good vibration reduction in the fuselage and gearbox. Increasing the number of sensors seemed to reduce the magnitude of control forces required for vibration minimisation. The choice of low vibratory level node location for sensor placement gave unsatisfactory results.

It is observed that sensor locations have a significant influence on the level of vibration reduction in fuselage structure.

## ACKNOWLEDGEMENT

Let me take this opportunity to express my deep gratitude to Dr V R Sule, for providing valuable guidance and encouragement throughout this work. His freshness of ideas and suggestions during our discussions gave direction to my work. I am much indebted to him for all the patience shown towards my many drawbacks.

I am very grateful to Dr C Venkatesan, who was always very keen and enthusiastic about this work. It was a pleasure to discuss various aspects of this work with him.

Words fail to express my love and gratitude to my dearest friend and sister, Maymol, who was *always there* when I needed her. Her acquaintance has truly enriched my life in more ways than one. I carry a huge bundle of warm loving memories of our time spent together.

Much gratitude is due to Dr Joseph John and Neena Chechy who gave me *a home away from home*. Their love and warmth strengthened me immensely. I will always be grateful to them for all their encouragement and support. I very much relished my friend Geetha's company. It was a joy to have studied along with her. Also, special thanks to Ajith and Balu, whose friendship I truly enjoyed and for helping me in so very many ways. It was a pleasure to have known Suja, Cini, Biju, Satheesh, Ritesh and Saju during my time spent in IIT. Thanks are also due to Sundar, Supriya and little Sandeep whose company I very much relished. I would also like to extend my thanks to Mr Uday Majumdar of control systems lab whose help and cooperation made much difference.

Words seem insufficient to express my love to my dear parents who lavished love and care on me. Special thanks to Bobby and Nutan for their love and concern. Thanks to all my dear ones who prayed tirelessly for me.

All my happiness I share with my dear half, Shibu, who was truly the *wind beneath my wings* for the past few months. What would have I done without all the love and encouragement he gave? Special thanks for all the cheer that the deluge of letters, phone calls, emails etc brought.

Above everything, all thanks to my Lord and Saviour Jesus Christ whose tender mercies made my IITK life truly blessed.

# Contents

List of Figures	iii
List of Tables	v
Nomenclature	vi
<b>1 INTRODUCTION</b>	<b>1</b>
1 1 Introduction To The Vibration Control Problem	1
1 2 Objectives Of The Present Study	3
1 3 Organisation Of The Thesis	4
<b>2 Design And Development of Control Laws For Vibration Minimisation</b>	<b>5</b>
2 1 Introduction	5
2 2 Description Of The Coupled Gearbox Fuselage System	5
2 3 Approach to Control Law Design	7
2 3 1 Algorithm for flexible/rigid body mode system decomposition	8
2 3 2 Algorithm for Model Order Reduction	9
2 3 3 Controller Design	11
2 3 4 Calculation of Control Forces	13
<b>3 RESULTS AND DISCUSSION</b>	<b>15</b>
3 1 Simulation Results For Various Choices Of Sensor Locations	15
3 1 1 Optimal Sensor Locations (Node Locations 8, 17, 23, 34 and 39)	15
3 1 2 Arbitrary Choice Of High Vibration Nodes (Node Locations 12, 16, 32, 33, and 38)	18
3 1 3 Arbitrary Choice Of Low Vibration Nodes (Node locations 6, 20, 28, 44, and 64)	19



3.1.4	Optimal Sensor Locations With A Tail Sensor (Node Locations 17, 23, 34, 39, and 64)	20
3.1.5	Seven Optimal Sensor Locations (Node Locations 8, 17, 23, 34, 39, 17, and 28)	20
4	Concluding Remarks	53
	Appendix A	55
	Appendix B	58
	Bibliography	61

# List of Figures

2 1	The Generalized 4 Block Plant	11
2 2	The Standard Block Diagram	12
2 3	The Closed Loop System	14
3 1	Coupled Gearbox Fuselage Dynamic Model	31
3 2	Baseline Finite Element Model of Helicopter Fuselage	32
3 3	Optimal Sensor Locations for Baseline Configuration of the Helicopter	33
3 4	Frequency Response of the Full Order Model for Nodes at 8, 17 23 34, 39	34
3 5	Frequency Response of the Reduced Order Model for Nodes at 8 17 23 34 39	35
3 6	Comparison of Frequency Response of the Full and Reduced Order Model (Node No 8)	36
3 7	Comparison of Frequency Response of the Full and Reduced Order Model (Node No 17)	37
3 8	Comparison of Frequency Response of the Full and Reduced Order Model (Node No 23)	38
3 9	Comparison of Frequency Response of the Full and Reduced Order Model (Node No 34)	39
3 10	Comparison of Frequency Response of the Full and Reduced Order Model (Node No 39)	40
3 11	Frequency Response of the Uncontrolled and Closed Loop Controlled Sys tem (Node No 8)	41
3 12	Frequency Response of the Uncontrolled and Closed Loop Controlled Sys tem (Node No 17)	42

3 13	Frequency Response of the Uncontrolled and Closed Loop Controlled System (Node No 23)	43
3 14	Frequency Response of the Uncontrolled and Closed Loop Controlled System (Node No 34)	44
3 15	Frequency Response of the Uncontrolled and Closed Loop Controlled System (Node No 39)	45
3 16	Comparison of Baseline and Closed Loop Controlled Vibratory Levels (Node Locations 8 17 23 34 39)	46
3 17	Comparison of Baseline and Open Loop Controlled Vibratory Levels (Node Locations 8 17 23 34 39)	47
3 18	Comparison of Baseline and Closed Loop Controlled Vibratory Levels (Node Locations 12, 16, 32 33, 38)	48
3 19	Comparison of Baseline and Closed Loop Controlled Vibratory Levels (Node Locations 6, 20 28, 44, 64)	49
3 20	Comparison of Baseline and Closed Loop Controlled Vibratory Levels (Node Locations 17 23 34, 39 64)	50
3 21	Comparison of Baseline and Closed Loop Controlled Vibratory Levels (Node Locations 8, 17, 23, 34, 39, 15 28)	51
3 22	Comparison of Baseline and Open Loop Controlled Vibratory Levels (Node Locations 8 17, 23 34, 39, 15, 28)	52

# List of Tables

3 1	Comparison of Baseline and Controlled Vibratory Levels	17
3 2	Control Forces for Optimal Sensor Locations (Closed Loop)	17
3 3	Control Forces for Optimal Sensor Location (Open Loop)	18
3 4	Control Forces for Arbitrary High Vibration Nodes (Closed Loop)	19
3 5	Control Forces for Arbitrary Low Vibration Nodes (Closed Loop)	20
3 6	Control Forces for Optimal Sensor and Tail Sensor Locations (Closed Loop)	21
3 7	Control Forces for 7 Optimal Sensor Locations (Closed Loop)	21
3 8	Control Forces for 7 Optimal Sensor Locations (Open Loop)	22
3 9	Eigenvalues of the Full System	23
3 10	Eigenvalues of the Flexible Mode System	25
3 11	Eigenvalues of the Rigid Body Mode System	27
3 12	Hankel Singular Values of the Flexible Mode System	28
3 13	Hankel Singular Values of the Reduced Order System	30

## Nomenclature

$[A]$ $[B]$ $[C]$	System matrix Control matrix and Output matrix respectively
$F_c^i$	Control force at the $i$ th gearbox support
$F_z(t)$	Vertical component of the hub load
$\{f\}$	Forcing function
$Nm$	Number of flexible modes of the fuselage
$NC$	Number of gearbox supports
$m_{CB}$	Mass of gearbox
$\tilde{z}_{CB}$	Rigid body vertical translation motion of gearbox
$\tilde{z}_F$	Rigid body vertical translation motion of fuselage
$\{\eta\}$	Modal coordinate vector of the elastic modes of fuselage
$\{\theta_{x_{CB}} \ \theta_{y_{CB}}\}$	Angular(roll and pitch) displacements of the gearbox
$\{\theta_{x_F} \ \theta_{y_F}\}$	Angular (roll and pitch) displacements of the fuselage
$H_\infty$	Haidy space
$\  \cdot \ _\infty$	Norm on $H_\infty$

# Chapter 1

## INTRODUCTION

### 1.1 Introduction To The Vibration Control Problem

In helicopters, controlling vibrations to acceptable limits is one of the key problems facing the rotorcraft designer. The time dependant aerodynamic and inertia loads acting on the rotor blades during forward flight cause vibration in helicopters. The harsh vibrational environment results in discomfort to pilot and crew and fatigue damage to the structure. In addition, vibration contributes to increased maintenance cost, difficulty in reading instruments and reduced effectiveness of weapons system. A comprehensive review on the sources of vibration and description of the sources of vibration and description of the methods for reducing vibration levels are given in [14] and [18].

The increasing demands for passenger transportation, high speed and high performance, improved manoeuvrability coupled with the need to improve system reliability and reduce maintenance costs has resulted in stringent requirements for vibrations. For present day helicopters, the general requirement is to have a maximum vibration level of 0.1g in the fuselage. With the adoption of stringent requirements (as given in [4]), it will become necessary in future to reduce vibratory levels below 0.05g or even lower.

The strategies employed for vibration control in helicopters can be broadly classified as passive or active control. The passive approach utilizes vibration absorbers and vibration isolation devices. Generally, their incorporation leads to increase in rotor weight and aerodynamic drag. Another passive approach is, careful structural dynamic design using

structural optimisation, aimed at minimising vibration in forward flight. The inability of the passive methods and devices to adapt to the wide operating conditions, represents a severe limitation.

The active control methodologies include HHC(Higher harmonic control), IBC(Individual blade control), ACF(Actively controlled flap) and ACSR(Active control of structural response) which has been described in detail in [9]. The higher harmonic pitch control of the blade provides a substantial reduction of vibratory levels in the fuselage but cause rotor blade stall at high speeds and require high power and low airworthiness criteria. ACF has been able to eliminate some of these drawbacks.

The ACSR scheme is based on the idea that in a linear system one can superimpose two independent response quantities such that total response is zero. See e.g. [3] and [19].

Vibration reduction is achieved by exciting the fuselage with actuators located at the gearbox support mountings such that the sum of the response of the airframe due to rotor loads and external excitation is reduced to a minimum. Refer [3],[20]. Ground and flight tests on the Westland 30 helicopter with the ACSR system, provided remarkable vibration reduction throughout the whole flight envelope explored. See [25]. The major advantages of ACSR are

- Ability to minimise vibration at specific fuselage location
- Simplicity and minimal impact on air worthiness requirements because vibration control is implemented entirely in the non rotating system
- Low power requirements
- It can operate at a multiplicity of frequencies

The analytical study on prediction and reduction of vibration in helicopter requires a realistic fuselage model. A 3 D finite element model of a helicopter fuselage, shown in fig (3.2) developed by Mangalick, et al, [23] has been used in the present study. The structural dynamic characteristics of this model resembles those of a realistic helicopter. The coupled gearbox fuselage dynamic model is given in fig (4.1).

The helicopter fuselage is described by 64 nodes (with 384 degrees of freedom) as shown in fig (3.2). Assuming that the rotor system consists of four blades, the vibratory hub loads will have a nondimensional excitation frequency of 4/rev. For the fuselage model, the nondimensional natural frequency of the 20th flexible mode is 6.4064 [Ref[21]] which is 50% more than the excitation frequency (4/rev) of the hub loads. Therefore the first 20 modes of the helicopter fuselage are considered in the vibration analysis. Since the vibratory level in the vertical direction ( $z$ ) in the fuselage is more predominant without loss of generality, it is assumed that the sensors measure only the  $z$  component of the fuselage vibration. The vibration control is performed only to minimise these  $z$  component of vibration.

The total number of degrees of freedom is 26 with 3 rigid body modes (pitch, heave, roll) of gear box, 3 rigid body modes (pitch, heave, roll) of fuselage and 20 flexible modes of fuselage. In state space, it is described by a 52 order system. For the present study, the vibratory response of the fuselage for only 4/rev disturbance excitation is considered.

## 1.2 Objectives Of The Present Study

The main problems addressed in this thesis are

- Formulation of a reduced order model, satisfactorily approximating the frequency response of the original system
- Formulation of a MIMO closed loop control scheme for vibration minimization, at the prescribed disturbance frequency (4/rev), using reduced order model
- Analyse the effectiveness of the closed loop control scheme in reducing the vibration in the fuselage, by incorporating in the full order model

The order reduction and closed loop control scheme are achieved by formulating a input output relation between 4 control inputs to a preselected set of a few sensor (say, 5 or 7) locations. These sensor locations have been chosen from an optimal set of 23 sensor



locations obtained in [21] following a procedure involving Fisher Information Matrix and Effective Independence Distribution vector. The optimal 23 sensor locations are as shown in fig (3.3).

## 1.3 Organisation Of The Thesis

The chapters in the thesis are organized as follows. Chapter 2 presents a description of equations of motion of the helicopters, followed by an introduction to the control law design. The algorithm for flexible/rigid body mode decomposition and the algorithm for model order reduction are described. This is followed by design of the controller, by factorisation theory using internal model principle for disturbance rejection.

Chapter 3 presents the results and discussion of the present study. Chapter 4 summarizes the results and gives concluding remarks on the present study.

# Chapter 2

## Design And Development of Control Laws For Vibration Minimisation

### 2 1 Introduction

For the design of controller for vibration reduction of helicopter at the disturbance frequency the necessary equations of motion describing the system are obtained from [21] As the initially given system is of high order [52 order state space system] a suitable reduced order model approximating the original system is obtained This necessitates the decomposition of the original system into two subsystems The flexible mode subsystem and the rigid body mode subsystem The flexible mode subsystem is then reduced, followed by formulating and implementing a strategy for disturbance rejection employing the well known internal model principle The control force used for vibration reduction is then calculated for the disturbance frequency

### 2 2 Description Of The Coupled Gearbox-Fuselage System

For a complete description of the coupled gearbox fuselage system for vibration analysis, we need equations of motion describing rigid body and flexible modes of the helicopter The equations of motion required are as follows The details are provided in [21]

- 1 The rigid body equations of motion of the gearbox It includes
  - Translational equations of motion

- Rotational equations of motion comprising of pitch and roll equations

2 The rigid body equations of motion of fuselage They are as above i.e

- Translational equations of motion
- Rotational equations of motion comprising of pitch and roll equations

3 The equations of motion of the elastic modes of the fuselage

These equations constitute the complete set of linear coupled differential equations used for vibration analysis

In state space form these equation can be written as

$$\{q\} = [A]\{q\} + [B]\{q\} + \{f\} \quad (2.1)$$

$$\{y\} = [C]\{q\} \quad (2.2)$$

where

$$\{q\} = \begin{Bmatrix} q_1 \\ q_2 \end{Bmatrix} \quad (2.3)$$

$$\{q_1\} = \begin{Bmatrix} Z_{GB} \\ \theta_{yGB} \\ \theta_{xGB} \\ \\ Z_F \\ \theta_{yF} \\ \theta_{xF} \\ \\ \eta_1 \\ \eta_2 \\ \eta_{Nm} \end{Bmatrix} \quad \{q_2\} = \{q_1\} \quad (2.4)$$

(6+Nm)x1

$$\{f\} = \begin{Bmatrix} 0_{(6+Nm) \times 1} \\ \frac{F(t)}{mGB} \\ 0 \\ 0 \end{Bmatrix}_{2(6+Nm) \times 1} \quad (2.5)$$

$$\{U\} = \begin{Bmatrix} F_c^1 \\ F_c^2 \\ F_c \end{Bmatrix}_{NC \times 1} \quad (2.6)$$

where  $Nm$  is the number of flexible modes of the fuselage and  $NC$  is the number of control inputs

Details of matrices  $[A]$   $[B]$  and  $[C]$  are provided in the Appendix of [21]  $[A]$  being a  $52 \times 52$  system matrix  $[B]$  a  $52 \times 4$  control matrix and  $[C]$  a  $65 \times 52$  output matrix

## 2.3 Approach to Control Law Design

### Introduction

The given 52 order system comprises of 46 flexible and 6 rigid body modes or zero frequency modes. The eigenvalues of the full system are as given in Table(3.9). The eigenvalues close to, or almost equal to zero, constitute the rigid body modes.

The given system is decomposed into parallel systems comprising of flexible and rigid body mode subsystems. The state space model of the decomposed system is given as

$$\begin{Bmatrix} x_1 \\ x_2 \end{Bmatrix} = \begin{bmatrix} A_1 & 0 \\ 0 & A_2 \end{bmatrix} \begin{Bmatrix} x_1 \\ x_2 \end{Bmatrix} + \begin{bmatrix} B_1 \\ B_2 \end{bmatrix} \begin{Bmatrix} U_1 \\ U_2 \end{Bmatrix} \quad (2.7)$$

$$\{y\} = [C_1 \quad C_2] \begin{Bmatrix} x_1 \\ x_2 \end{Bmatrix} \quad (2.8)$$

where  $(A_1, B_1, C_1)$  is the 46 order flexible subsystem and  $(A_2, B_2, C_2)$  is the 6th order rigid body system. The eigenvalues of  $A_1$  and  $A_2$  are given in table(3.10) and table(3.11). The eigen values of  $A_1$  are all in the left half complex plane and hence it is a stable system.

and eigenvalues of  $A_2$  are all nearly zero with one of the values, shown as negative value which is due to numerical computational error

For vibration control only the flexible modes are considered which have natural frequency close to disturbance frequency. The rigid body system is almost uncontrollable and hence is not considered for controller design.

### 2.3.1 Algorithm for flexible/rigid body mode system decomposition

This decomposition requires finding a state coordinate transformation which results in matrix  $A$  being block diagonal, each of the diagonal blocks having the required eigenvalues. See [15, 22]

This problem is solved as

- first reducing the matrix  $A$  to schur form
- secondly reordering the unordered schur form so that the eigenvalues (diagonal elements) are grouped as required
- thirdly reducing the remaining off diagonal blocks to zero without disturbing the diagonal blocks

The schur form of  $A$  matrix is obtained by finding a unitary similarity transformation say  $S$ , using the QR algorithm. Refer [22]

The matrix  $A$  is reduced to its schur form as

$$A_s = S^H A S = \begin{bmatrix} A_{11} & A_{12} \\ 0 & A_{22} \end{bmatrix}$$

where  $A_{11}$  and  $A_{22}$  are upper triangular matrices and their dimensions are determined by the required state dimensions of the parallel subsystems. After this transformation the eigenvalues are distributed randomly between  $A_{11}$  and  $A_{22}$ . A transformation matrix say  $G$ , which distributes them as needed is obtained by means of simple bubble sorting via givens rotation, which interchanges a pair of adjacent diagonal elements of  $S^H A S$  [15]. After this, we have

$$T = G^H A_s G = \begin{bmatrix} T_{11} & T_{12} \\ 0 & T_{22} \end{bmatrix}$$

where  $T_{11}$  and  $T_{22}$  have the 46 flexible mode and 6 rigid body mode eigen values respectively

A further state coordinate transformation to reduce  $T_{12}$  to zero is found This is done using a transformation matrix of the form,

$$Y = \begin{bmatrix} I & Y_{22} \\ 0 & I \end{bmatrix}$$

in which dimensions of the blocks are the same as T  
As,

$$Y^{-1}TY = \bar{T} = \begin{bmatrix} T_{11} & 0 \\ 0 & T_{22} \end{bmatrix}$$

Then

$$TY = Y\bar{T}$$

Which leads to the sylvester equation,

$$T_{11}Y_{12} - Y_{12}T_{22} = -T_{12}$$

which is solved for  $Y_{12}$  Refer [22]

The final coordinate trasfermation required to decompose the original system  $[A,B,C D]$  is

$$R = GY$$

so that the decomposition is obtained by simply partitioning the matrices of the realisation  $[R^{-1}AR, R^{-1}B, CR, D]$

## 2 3 2 Algorithm for Model Order Reduction

The stable 46th order flexible mode subsystem is now considered for order reduction

The main objective of order reduction is to,

- Find a reduced order model that reasonably approximates the frequency response of the original system upto 4/rev
- Secondly the controller design for reduced system should effectively stabilise and control the full order system as well

Balanced realisation being one of the best methods for reducing the order of flexible space structures, having closely placed eigenvalues Refer [10] we find the balanced coordinates for the given 46 order subsystem

A balanced realisation  $[A_b \ B_b \ C_b \ D_b]$  is one for which the controllability and observability grammians which are solutions of the equations

$$A_b W_r + W_r A_b^T + B_b B_b^T = 0$$

$$A_b^T W_b + W_b A_b + C_b^T C_b = 0$$

are equal, that is,

$W_r = W_o = \Sigma$ , a diagonal matrix Refer [8 11,17]

The state coordinate transformation for this is found using the algorithm in [13] and is briefly outlined below

- Compute cholesky factors of the grammians
- Let  $L_r$  and  $L_o$  denote the lower triangular cholesky factors of grammians  
 $W_r = L_r L_r^T$  ,  $W_o = L_o L_o^T$
- Compute singular value decomposition of the product of cholesky factors  
 $L_o^T L_r = U \Lambda V^T$   
 where U and V are unitary matrices and  $\Lambda$ , a diagonal matrix
- Form the balancing transformation  
 $T = L_r V \Lambda^{-\frac{1}{2}}$

- For the balanced state space realisation

$$A = T^{-1}AT \quad B = T^{-1}B \quad C = CT$$

we find that

$$T^{-1}W_rT^{-1} = T^TW_oT = \Lambda$$

After this, by observing the hankel singular values of the full system as given in Table(3 12) the part which contained the lowest singular values i.e. which are most weakly coupled to the inputs and outputs were truncated. It was found that an 18th order model whose hankel singular values are given in Table(3 13) was sufficient to satisfy the objectives as mentioned earlier.

### 2 3 3 Controller Design

The reduced order model is used for controller design. For this we use the standard controller parametrisation of the factorisation theory (Appendix A). We initially consider the system with 4 control inputs, One disturbance input and 5 outputs. This system is represented in standard 4 block form as

where

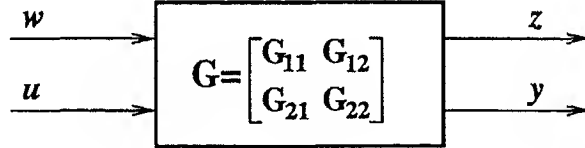


Figure 2 1 The Generalized 4-Block Plant

$w$  = exogenous input consisting of disturbance signal

$u$  = control signal

$z$  = output to be controlled

$y$  = measured output

A feedback controller  $C$  is attached to the plant to form the feedback system shown below

The standard problem is to find a real, rational proper  $C$  to minimize the  $H_\infty$  norm of  $T_{zw}$  the transfer matrix from  $w$  to  $z$  under the constraint that  $C$  stabilise  $G$ . Refer [24]



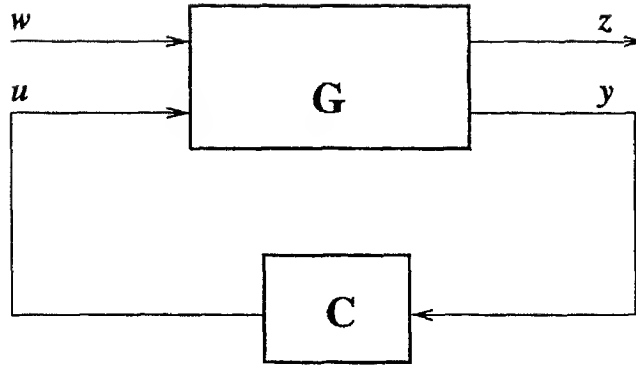


Figure 2.2 The Standard Block Diagram

Using factorisation theory as explained in Appendix B, the transfer matrix  $T_{zw}$  can be written as

$$T_{zw} = T_1 - T_2 Q T_3$$

where

$T_1$ ,  $T_2$  and,  $T_3$

are transfer matrices obtained from the plant and  $C(s)$  as given in Appendix B

For asymptotic disturbance rejection of the sinusoidal signal at 4/rev, we consider the internal model principle. See [6,15,16,26]. According to internal model principle, we can obtain asymptotic disturbance rejection by incorporating in the feedback path, a suitable reduplicated model of the dynamic structure of disturbance signal. The purpose of the internal model is to supply closed loop transmission zeroes which cancel the poles of the disturbance signal.

To attain this using the model matching criterion, the values of  $T_1$ ,  $T_2$  and  $T_3$  matrices at  $s = \pm j4$  is found such that

$$T_1(\pm j4) - T_2(\pm j4)Q(\pm j4)T_3(\pm j4) = 0$$

The value of  $Q$  at  $s = \pm j4$  which satisfies above equation is found out. They are complex conjugates of each other.

The state space matrices for  $Q$  are found out by equating each term of  $Q(\pm j4)$  by

transfer functions of the form

$$\frac{s^2+as+bs}{(s+1)^2}$$

where a and b are found by solving the two equations given below

Solving, for  $s = j4$

$$\frac{s^2+as+bs}{(s+1)^2} = \text{value of respective term at } Q(j4)$$

and for  $s = -j4$

$\frac{s^2+as+bs}{(s+1)^2} = \text{value of respective term at } Q(-j4)$  we obtain the values of a and b After the transfer matrix of Q is found out the stable state space block observer form of Q was determined as given in [12] The Q so obtained was used in obtaining the stabilizing controller

The controller designed for 18th order plant was found to stabilise the 46th order plant without introducing any new unstable modes when used along with the full system

## 2 3 4 Calculation of Control Forces

For the calculation of control forces, required to be applied by the actuators at the gear box mountings, we consider the state space description of the helicopter system and controller as given below

$$x_p = Ax_p + Bu_p + f$$

Plant

$$y_p = Cx_p + Du_p$$

$$x_c = A_c x_c + B_c u_c$$

Controller

$$y_c = C_c x_c + D_c U_c$$

$y_p$  is the plant output, representing the vibration measurement at 5 sensor location for a disturbance frequency f,  $u_p$  is the input to the plant, representing the 4 control forces applied  $u_c$  and  $y_c$  are the respective controller inputs and outputs respectively

Now,  $y_p = u_c$

and

$$y_c = -u_p$$

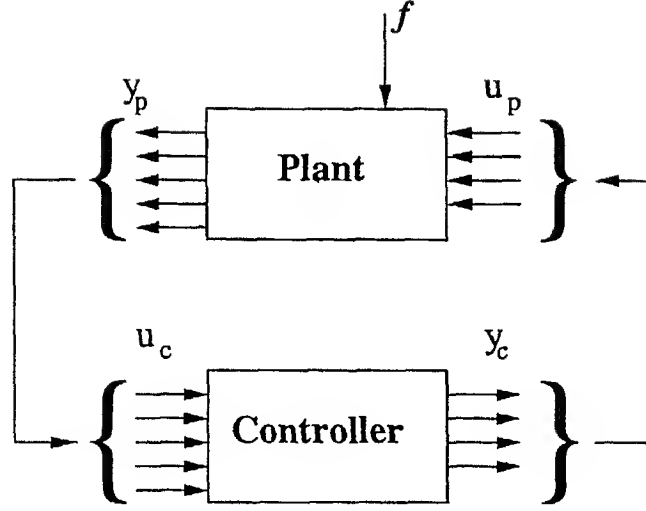


Figure 2.3 The Closed Loop System

$y_p$  is calculated as the open loop vibration (ie,  $u_p = 0$ ) of the system for 4/rev input disturbance frequency,  $f = 1$  e,

$$y_p = [C_p[A_p - \nu w I]^{-1}B_p + D_p]f$$

where,  $w = 4/\text{rev}$  As  $y_p = u_c$ ,

From this, knowing the controller description, the controller output force is calculated as

$$y_c = [C_c[A_c - \nu w I]^{-1}B_c + D_c]u_c$$

$u_p = y_c$ , gives the control force required for vibration minimisation

Thus the control laws were formulated using the above given algorithms and the stabilising controller designed for vibration minimisation, using the reduced order model

# Chapter 3

## RESULTS AND DISCUSSION

This chapter deals with the presentation of results of control laws that were discussed in the previous chapter. The results of these studies are presented in the following sections. In the first section, a set of 5 sensor locations, chosen from an optimal set of locations as given in Ref [21] is considered. The results of the closed loop control scheme and open loop control design, (as in [21]) are analysed. The second and third sections, deal with arbitrary choices of high and low vibration node locations respectively, for closed loop control. In the fourth section, a sensor at the tail portion of the fuselage is considered along with optimal sensor node locations. Finally 7 sensor locations from the optimal set is considered for vibration minimisation study.

### 3.1 Simulation Results For Various Choices Of Sensor Locations

#### 3.1.1 Optimal Sensor Locations (Node Locations 8, 17, 23, 34 and 39)

##### Closed Loop Control Scheme

The data for mathematical model of the helicopter system in the state space form was taken from Ref [21]. For the initial study, optimal sensor locations at nodes 8, 17, 23, 34 and 39 which have high levels of vibration are chosen. The actuators are placed at nodes 39, 48, 46 and 37. The

given 52 order system is decomposed into 46 and 6th order subsystems as explained in sec (2 3 1) The 46th order system considered for controller design is a stable system Balanced realisation based model order reduction technique as explained in sec (2 3 2) is employed to transform the given system into its balanced state space coordinates The hankel singular values of the 46th order system as given in table[3 12] gives an idea of the number of modes that are comparatively strongly coupled to the input and output

By trial, the system was initially truncated to a 10th order model The 10th order system sufficiently approximated the frequency response of the original full system But after controller design it is seen that the controller could not effectively stabilise the full order system This could be because of spillover instability which is caused by the inadvertent excitation of the truncated or residual modes and their unwanted contribution to the sensed output Refer [1] and [5] The size of the reduced order model is increased one at a time till stability was attained An 18th order model is found that satisfactorily approximated the frequency response of the full system and also stabilised the full system for the chosen 5 sensor locations This can be seen by comparing fig [3 4] and fig[3 5] The individual comparison for all the 5 sensors are shown in fig[3 6] to fig[3 10] The lower frequency ranges gave a better match as compared to higher frequency ranges as the helicopters natural frequencies are all in (1/rev 6/rev) range

Following the procedure described in chapter 2, the controller designed is of 22nd order The controller designed for reduced order model is incorporated in the feedback loop of the full system and the vibratory levels is calculated at all nodes The vibratory levels at all the 5 chosen locations after control as compared to the baseline values is shown individually from fig [3 11] to fig [3 15] Their dB values are as shown in the table(3 1) given below

The comparison between baseline and controlled vibration level at all the 64 nodes is shown in fig[3 16] The node location 0 indicates the sensor placed at the centre of gravity of the gearbox The peak vibration g level in the baseline configuration of the helicopter is 0 2696g at node location 33 and lowest value of vibration is at node 57 of 0 00017g The closed loop design, gives maximum vibration at node location 33 of 0 0364g which is

Node No	Baseline dB value	Closed loop dB value
8	24 5398	37 3724
17	14 1060	128 157
23	21 1613	31 1831
34	13 3981	29 6488
39	21 7099	33 4949

Table 3 1 Comparison of Baseline and Controlled Vibratory Levels

lower than peak baseline value. Vibration in the tail portion of the fuselage ( i.e. nodes above 50) is seen to be more after closed loop design. For example at node location 64, there is a increase in the vibration g level from the baseline value of 0 0032g to 0 0145g. This could be because there is no sensor chosen from the tail region. Vibration at the gearbox i.e., node 0 is seen to reduce from the baseline value of 0 0598g to 0 01864g.

The control forces are calculated as per the procedure given in sec(2 3 4). The magnitude and phase angles of forces applied at each of the actuator nodes is given in table(3 2).

Node No	Magnitude ( $10 \times 10^3$ )	Phase angle (deg )
39	1 9218	154 19
48	2 9892	-154 53
46	0 8335	52 50
37	0 5604	45 77

Table 3 2 Control Forces for Optimal Sensor Locations (Closed Loop)

### Open Loop Control Scheme

An open loop control formulation is also done for the same set of five sensor locations

from the optimal set, as per the design given in [21] After open loop control the vibration is seen to reduce significantly at all nodes, other than the gearbox where there is a increase from baseline value of 0.0598g to 0.0624g The comparison between open loop-controlled values and the baseline values is shown in fig(3.17) The maximum level of vibration after control is at node location 42 of 0.00054g which is quite lower than the peak baseline value of 0.2696g at node 33

The control forces required are much lower than that for closed loop control scheme The magnitude and phase angles of the control forces are given below in table(3.3)

Node No	Magnitude	Phase angle (deg )
39	3.7521	179.21
48	3.7567	179.21
46	3.7558	179.48
37	3.7580	179.35

Table 3.3 Control Forces for Optimal Sensor Location (Open Loop)

### 3.1.2 Arbitrary Choice Of High Vibration Nodes (Node Locations 12, 16, 32, 33, and 38)

For the next study another set of 5 arbitrary sensor locations at 12, 16, 32, 33, 38 are chosen They are high vibratory level node locations but not optimal as per Ref [21] A similar procedure as explained in earlier section is carried out A 20th order model was found to sufficiently approximate the full system This gives a 24th order controller The comparison between baseline and controlled vibration level for the the full system is shown in fig(3.18) The maximum vibration is observed at node location 17 of 0.0326g which is lesser than the peak baseline level of 0.2696g at node 33 In the tail region ,there is seen to be an increase in the level of vibration For example, at node location 64 ,the vibration increases from baseline value of 0.0032g to 0.017808g In the gearbox, there is reduction in vibration from a baseline level of 0.0598g to 0.01359g after control Thus the

high vibratory nodes are seen to be effective for vibration reduction The control forces are almost similar to forces for optimal sensor locations The magnitude and phase angle of control forces are as given in table(3 4)

Node No	Magnitude ( $1.0 \times 10^3$ )	Phase angle (deg )
39	1 1754	150 54
48	1 4224	137 08
46	1 4095	70 38
37	0 9981	63 31

Table 3 4 Control Forces for Arbitrary High Vibration Nodes (Closed Loop)

### 3 1 3 Arbitrary Choice Of Low Vibration Nodes (Node locations 6, 20, 28, 44, and 64)

A similar study was carried out for another set of arbitrary 5 sensor locations having low vibratory levels Here a 30th order model was needed to sufficiently approximate the full order system The controller is of 34th order

The comparison between baseline and controlled vibration level for the full system is shown in fig(3 19) The maximum vibration is observed at node 33 of 0 2205g which is close to the peak baseline value of 0 2696g At the majority of the nodes the vibration after control is seen to be more than the baseline values This may be because the sensor measurements of the low vibratory nodes might have been inaccurate resulting in inaccurate calculation of control forces There is an increase in the gearbox vibratory level from the baseline value of 0 0598g to 0 0818g

It is not safe to choose low vibratory level nodes as sensor location points for vibration reduction The magnitude and phase of the control forces are as given in table(3 5)



Node No	Magnitude	Phase angle (deg )
39	43 052	3 86
48	36 73	-1 96
46	30 47	7 30
37	85 52	0 10

Table 3 5 Control Forces for Arbitrary Low Vibration Nodes (Closed Loop)

### 3 1 4 Optimal Sensor Locations With A Tail Sensor (Node Locations 17, 23, 34, 39, and 64)

For this study, the same initial set of optimal sensor locations were chosen with one of the nodes 8, replaced by a sensor chosen at the tail of the fuselage i.e node 64. A 22nd order model approximates sufficiently the full order system.

The comparison between baseline and controlled vibration level for the full system is shown in fig (3 20). The maximum vibration is observed at node 38 of 0 02743g. Vibration is seen to be lowered at all the nodes. Specially in the tail region, there is seen to be much reduction as compared to earlier choices. For example at node location 55, there is seen to be reduction from the baseline value of 0 00367g to 0 00041g. This could be because of the presence of a sensor at the tail region along with other high vibration nodes.

The control forces calculated here are lower than the 1st and 2nd choices of sensor locations. They are as shown in table(3 6).

### 3 1 5 Seven Optimal Sensor Locations (Node Locations 8, 17, 23, 34, 39, 17, and 28)

#### Closed Loop Control Scheme

For this study a set of 7 sensor locations from the optimal set were chosen and the controller designed as per the earlier procedure. A 24th order system approximates the full system.

Node No	Magnitude ( $1.0 \times 10^3$ )	Phase angle (deg )
39	0.8474	165.85
48	1.9157	165.17
46	0.1161	115.18
37	0.1607	175.32

Table 3.6 Control Forces for Optimal Sensor and Tail Sensor Locations (Closed Loop)

The comparison between baseline and controlled vibration levels is shown in fig(3.21). The peak baseline vibration level is 0.2697g at node location 33. The peak controlled response is 0.0379g at node location 62. At the gearbox, there is a reduction in vibration from the baseline value of 0.05988g to 0.0218g. In the tail region for example at node 64, there is an increase in vibration from the baseline value of 0.00321g to 0.03749g.

The control forces are as shown in table(3.7). The magnitude of control force is seen to have been lowered in the case of 7 sensors by a factor of 10 as compared to optimal 5 sensor locations.

Node No	Magnitude ( $1.0 \times 10^2$ )	Phase angle (deg )
39	3.4388	11.57
48	5.3327	12.83
46	0.5525	84.96
37	0.4289	59.77

Table 3.7 Control Forces for 7 Optimal Sensor Locations (Closed Loop)

### Open Loop Control Scheme

An open loop scheme formulation is again done for the same set of 7 optimal sensor locations, as per the design given in [21]. There is a significant reduction in vibration at all nodes except at the gearbox after control. The comparison between baseline and open loop controlled vibratory levels is shown in fig (3.22). At the gearbox i.e., node 0,

there is an increase in vibration from baseline value of 0.0598g to 0.06249g. Other than gearbox, the peak vibration is at node location 42 of 0.00028g, which is quite lower than the baseline value. The control forces required are similar to that required for the open loop formulation for 5 optimal sensor locations. The magnitude and phase angles of the control forces are as given in table(3.8)

Node No	Magnitude	Phase angle (deg )
39	3.7553	-179.47
48	3.7553	-179.69
46	3.7561	179.47
37	3.7567	179.44

Table 3.8 Control Forces for 7 Optimal Sensor Locations (Open Loop)

Thus, for various choices of the sensor locations, the control laws designed as per the algorithms explained in Chapter 2 were implemented and the results analysed.

Table 3 9 Eigenvalues of the Full System

S No	Eigen values
1	0 08875102976272 +17 29791108351503i
2	0 08875102976272 17 29791108351503i
3	0 02795818992943 +11 93083803276192i
4	0 02795818992943 11 93083803276192i
5	0 02800282165061 +12 30482819641770i
6	0 02800282165061 12 30482819641770i
7	0 03475416128688 + 7 05896159053937i
8	0 03475416128688 7 05896159053937i
9	0 03069535817620 + 6 13029696397045i
10	0 03069535817620 6 13029696397045i
11	0 03189076637836 + 5 82440867391609i
12	0 03189076637836 5 82440867391609i
13	0 03291029354580 + 5 53104714394176i
14	0 03291029354580 5 53104714394176i
15	0 02645884964234 + 5 44131232662959i
16	0 02645884964234 5 44131232662959i
17	0 02529607303838 + 4 92342188521718i
18	0 02529607303838 4 92342188521718i
19	0 02487619896223 + 4 79801229595323i
20	0 02487619896223 4 79801229595323i
21	0 02290578844185 + 4 39551765863855i
22	0 02290578844185 4 39551765863855i
23	0 02422156490082 + 4 76665773658356i
24	-0 02422156490082 4 76665773658356i
25	0 02234539199842 + 4 42907155283225i
26	0 02234539199842 4 42907155283225i
	Contd

S No	Eigen values
27	0 01984470001224 + 3 47435173914139i
28	0 01984470001224 3 47435173914139i
29	0 02380946872847 + 3 70094095012000i
30	0 02380946872847 3 70094095012000i
31	0 00484154758626 + 0 66366775694405i
32	0 00484154758626 0 66366775694405i
33	0 00408480616817 + 0 81456693456129i
34	0 00408480616817 0 81456693456129i
35	0 01526006344587 + 3 05898620442318i
36	0 01526006344587 3 05898620442318i
37	0 01463144712625 + 2 24567321755696i
38	0 01463144712625 2 24567321755696i
39	0 01091992240451 + 2 19632306442407i
40	0 01091992240451 2 19632306442407i
41	0 01329022673454 + 2 63113636358172i
42	0 01329022673454 2 63113636358172i
43	0 01238520927406 + 2 38374970141317i
44	-0 01238520927406 2 38374970141317i
45	0 01308997918679 + 2 60197904001544i
46	0 01308997918679 2 60197904001544i
47	0 00000000000000 + 0 00000006580385i
48	0 00000000000000 0 00000006580385i
49	0 00000000000000 + 0 00000003886751i
50	0 00000000000000 0 00000003886751i
51	0 00000003638915
52	0 00000003638915

Table 3 10 Eigenvalues of the Flexible Mode System

S No	Eigen values
1	0 08875102976282 +17 29791108351510i
2	0 08875102976282 17 29791108351510i
3	0 02800282165060 +12 30482819641770i
4	0 02800282165060 12 30482819641770i
5	0 02795818992936 +11 93083803276182i
6	0 02795818992936 11 93083803276182i
7	0 03475416128689 + 7 05896159053937i
8	0 03475416128689 7 05896159053937i
9	0 03069535817621 + 6 13029696397046i
10	0 03069535817621 6 13029696397046i
11	0 03189076637836 + 5 82440867391611i
12	0 03189076637836 5 82440867391611i
13	0 03291029354579 + 5 53104714394177i
14	0 03291029354579 5 53104714394177i
15	0 02645884964233 + 5 44131232662960i
16	0 02645884964233 5 44131232662960i
17	0 02529607303838 + 4 92342188521718i
18	0 02529607303838 4 92342188521718i
19	0 02487619896223 + 4 79801229595323i
20	0 02487619896223 4 79801229595323i
21	0 02422156490082 + 4 76665773658357i
22	0 02422156490082 4 76665773658357i
23	0 02290578844186 + 4 39551765863862i
24	0 02290578844186 4 39551765863862i
	Contd

S No	Eigenvalues
25	-0 02234539199843 + 4 42907155283226i
26	-0 02234539199843 4 42907155283226i
27	0 00484154758625 + 0 66366775694405i
28	0 00484154758625 0 66366775694405i
29	0 02380946872847 + 3 70094095012000i
30	0 02380946872847 3 70094095012000i
31	0 01984470001225 + 3 47435173914146i
32	0 01984470001225 3 47435173914146i
33	0 00408480616817 + 0 81456693456129i
34	0 00408480616817 0 81456693456129i
35	0 01526006344587 + 3 05898620442318i
36	0 01526006344587 3 05898620442318i
37	0 01463144712629 + 2 24567321755691i
38	-0 01463144712629 2 24567321755691i
39	0 01091992240451 + 2 19632306442407i
40	0 01091992240451 2 19632306442407i
41	0 01329022673455 + 2 63113636358170i
42	0 01329022673455 2 63113636358170i
43	0 01238520927406 + 2 38374970141317i
44	0 01238520927406 2 38374970141317i
45	0 01308997918679 + 2 60197904001544i
46	0 01308997918679 2 60197904001544i

Table 3 11 Eigenvalues of the Rigid Body Mode System

S No	Eigenvalues
1	0 000000000000004 + 0 00000007234537i
2	0 000000000000004 0 00000007234537i
3	0 000000000000000 + 0 00000001636733i
4	0 000000000000000 0 00000001636733i
5	0 00000002792489
6	-0 00000002792489



Table 3 12 Hankel Singular Values of the Flexible Mode System

S No	Hankel Singular values
1	0 50020032528298
2	0 49787295252775
3	0 39792717752109
4	0 39404491912856
5	0 35759304563833
6	0 35421141956328
7	0 34479476287702
8	0 34130683900409
9	0 29945680703380
10	0 29678280169811
11	0 29173934551814
12	0 29043391374987
13	0 25459758631574
14	0 25194694270086
15	0 22468950975344
16	0 22362607838112
17	0 17680269962824
18	0 17486793266184
19	0 12996833234765
20	0 12909073516741
	Contd

S No	Hankel Singular values
21	0 12542702992093
22	0 12419371688954
23	0 12303598050017
24	0 12180838112860
25	0 09296523656489
26	0 09162702036468
27	0 08657951501950
28	0 08566547809310
29	0 07624444932034
30	0 07547726648661
31	0 05103122671086
32	0 05027246928071
33	0 04351223375414
34	0 04331785763777
35	0 03378337083105
36	0 03370061818543
37	0 02159690395851
38	0 02146641949637
39	0 01790822070468
40	0 01772367433794
41	0 01556089680591
42	0 01543070638160
43	0 00223841030348
44	0 00221655909497
45	0 00213216554543
46	0 00211230529396

Table 3 13 Hankel Singular Values of the Reduced Order System

S No	Hankel Singular values
1	0 50008795899589
2	0 49775726294606
3	0 39792699404819
4	0 39404315404613
5	0 35768824775163
6	0 35419377218320
7	0 34477363921226
8	0 34128237140741
9	0 29205071328056
10	0 28869493786649
11	0 25465993779617
12	0 25208554185246
13	0 17677949506505
14	0 17482638374724
15	0 12314452287337
16	0 12191603548932
17	0 09301425910005
18	0 09167333022519

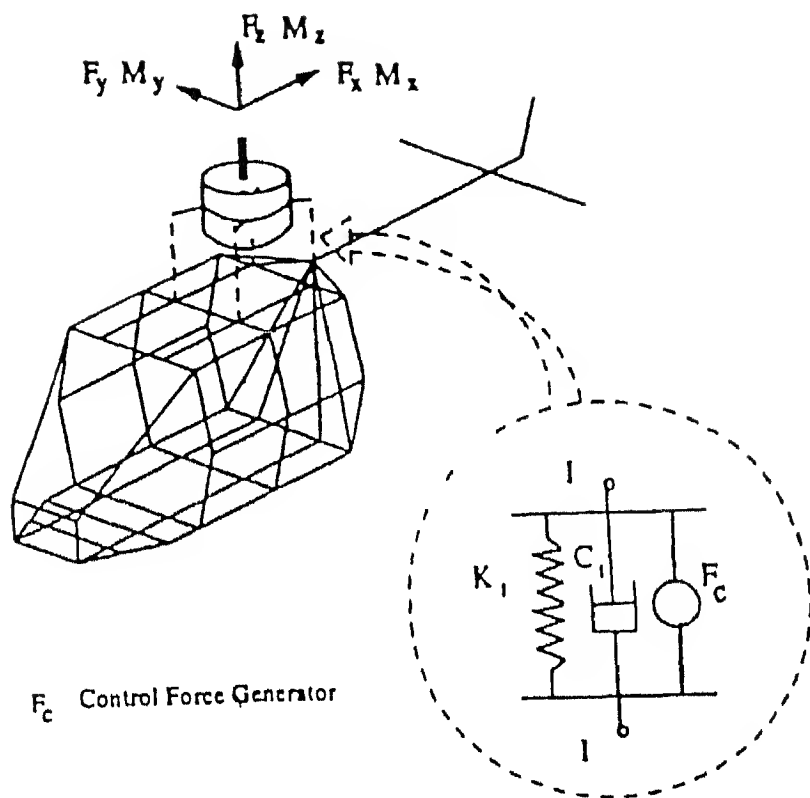


Figure 3 1 Coupled Gearbox Fuselage Dynamic Model

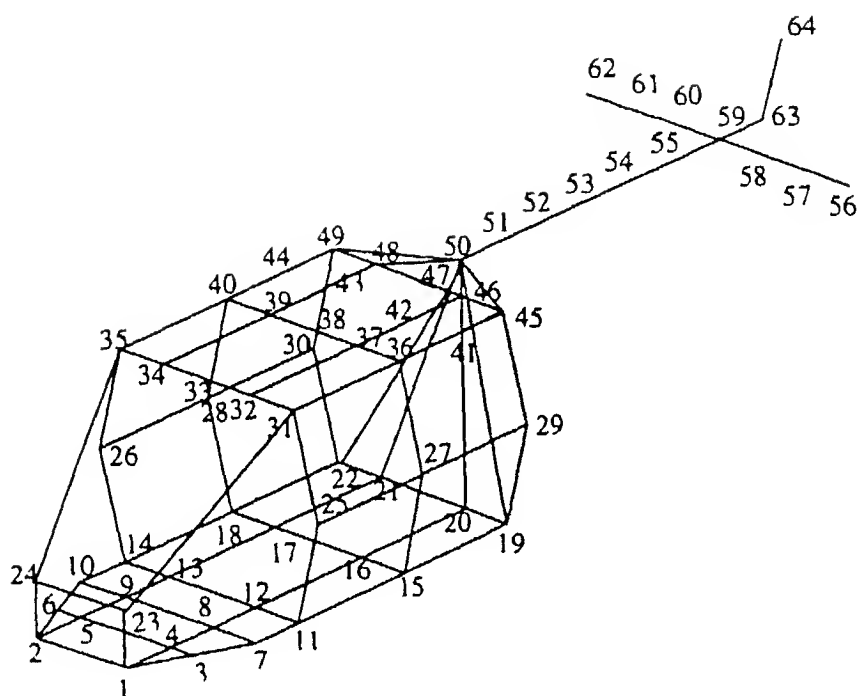


Figure 3 2 Baseline Finite Element Model of Helicopter Fuselage

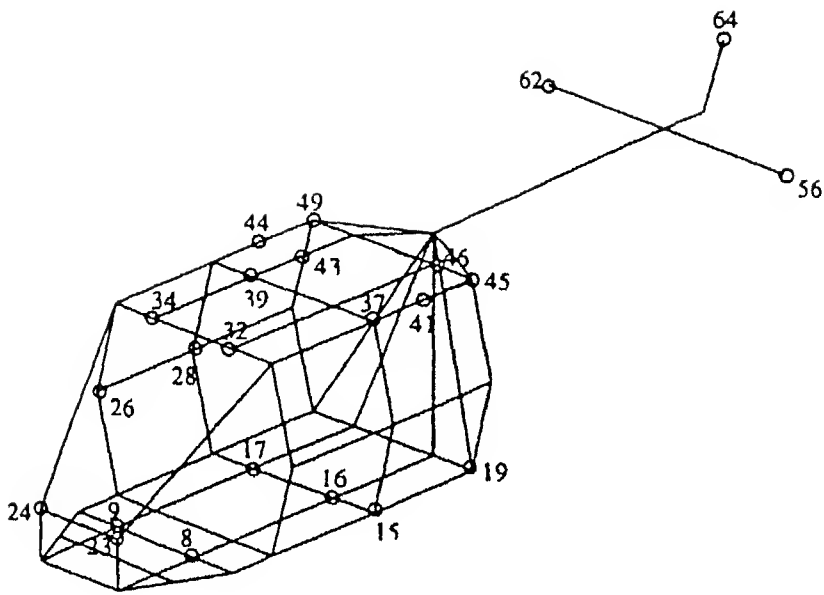


FIGURE 3.3 Optimal Sensor Locations for Baseline Configuration of the Helicopter

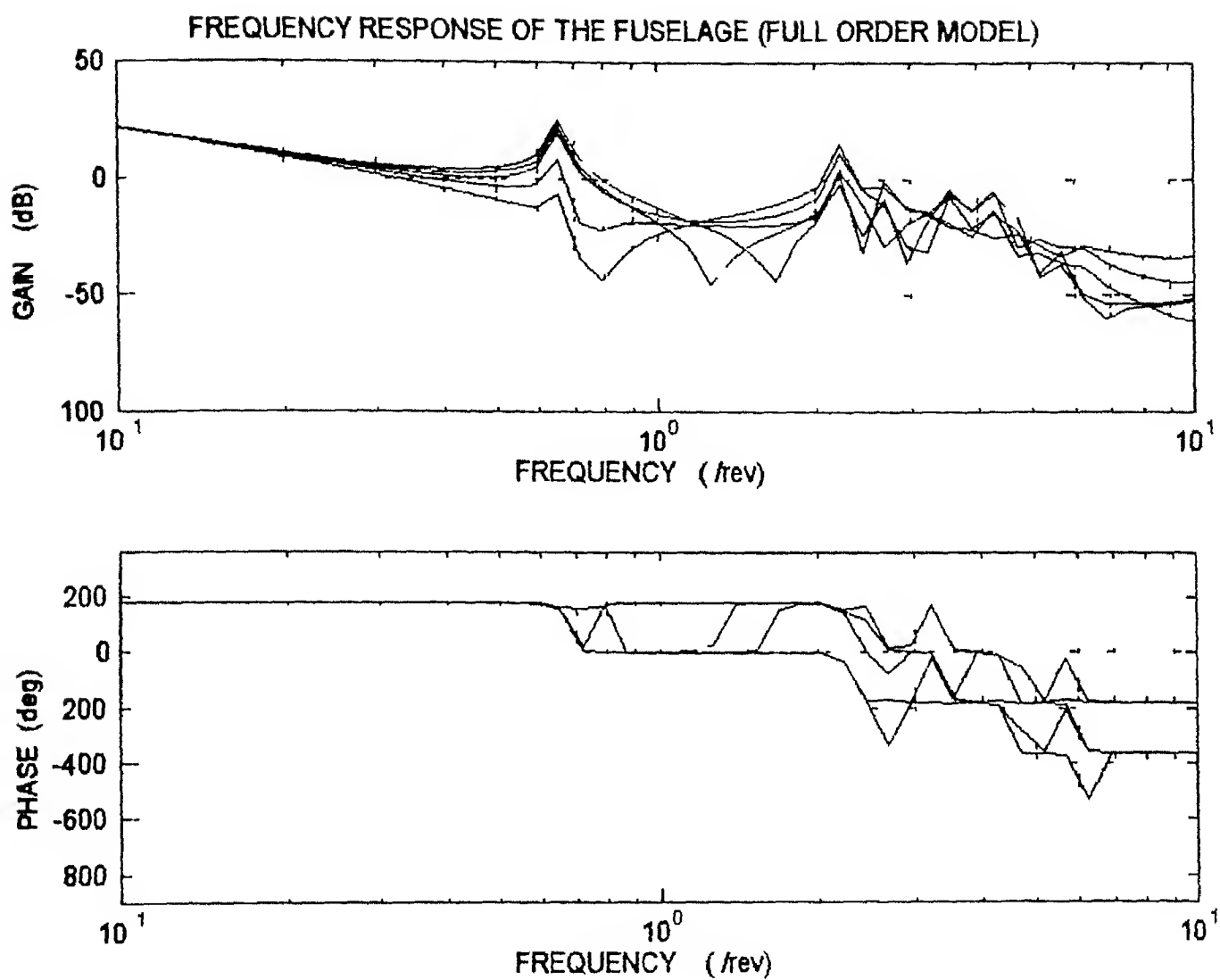


Figure 3.4 Frequency Response of the Full Order Model for Nodes at 8, 17, 23, 34, 39

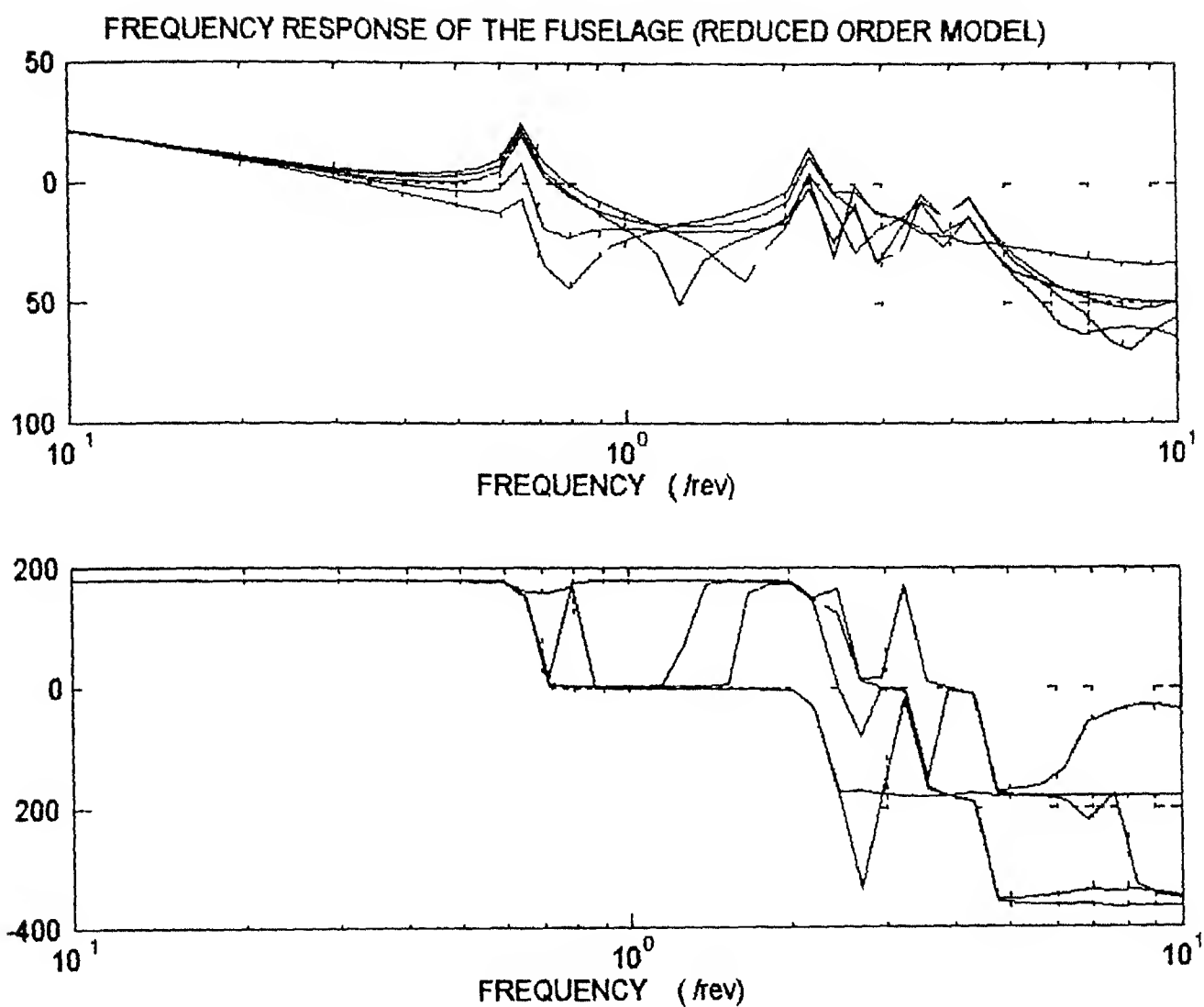


Figure 3 5 Frequency Response of the Reduced Order Model for Nodes at 8, 17, 23, 34, 39



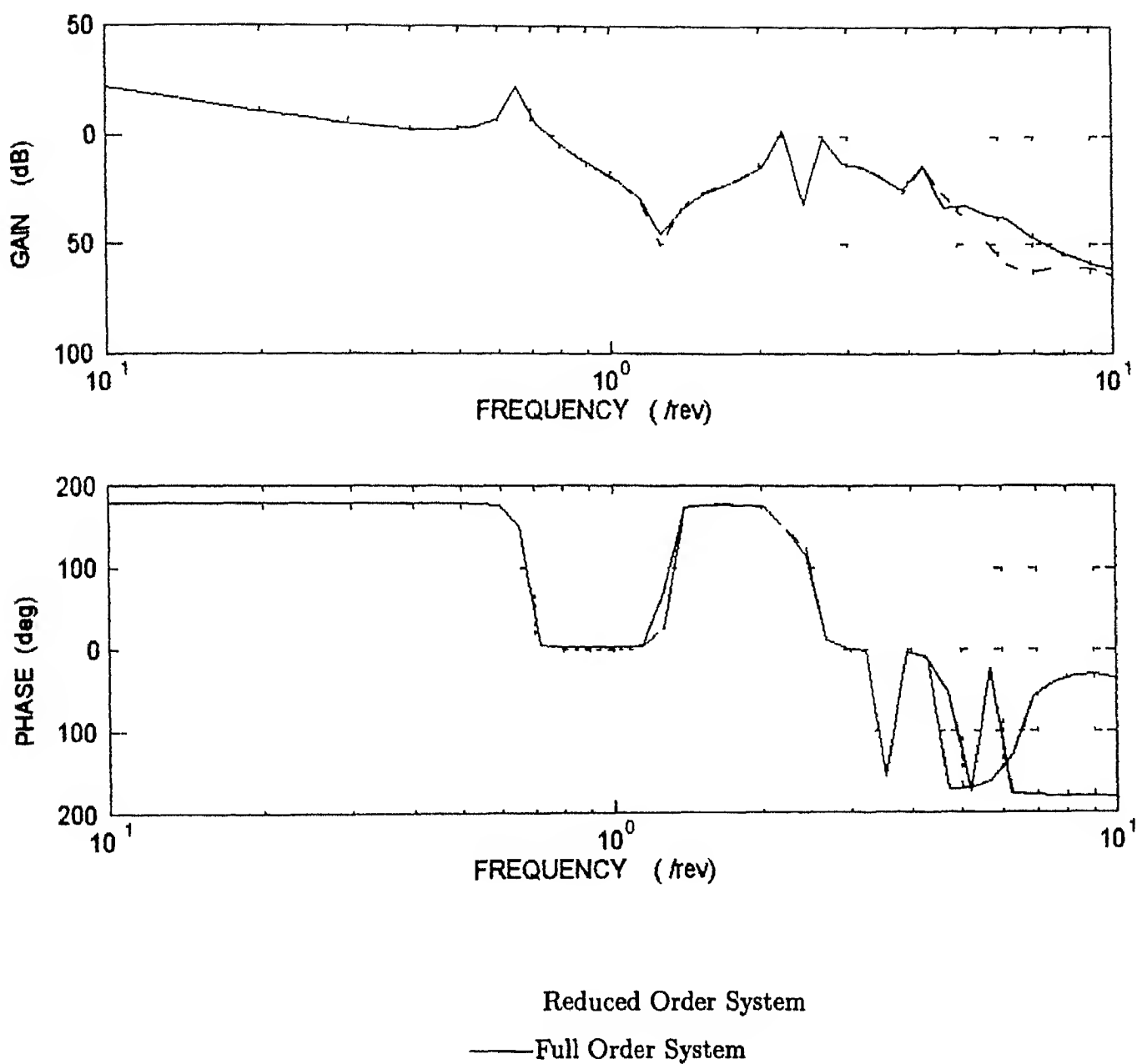


Figure 3.6 Comparison of Frequency Response of the Full and Reduced Order Model (Node No 8)

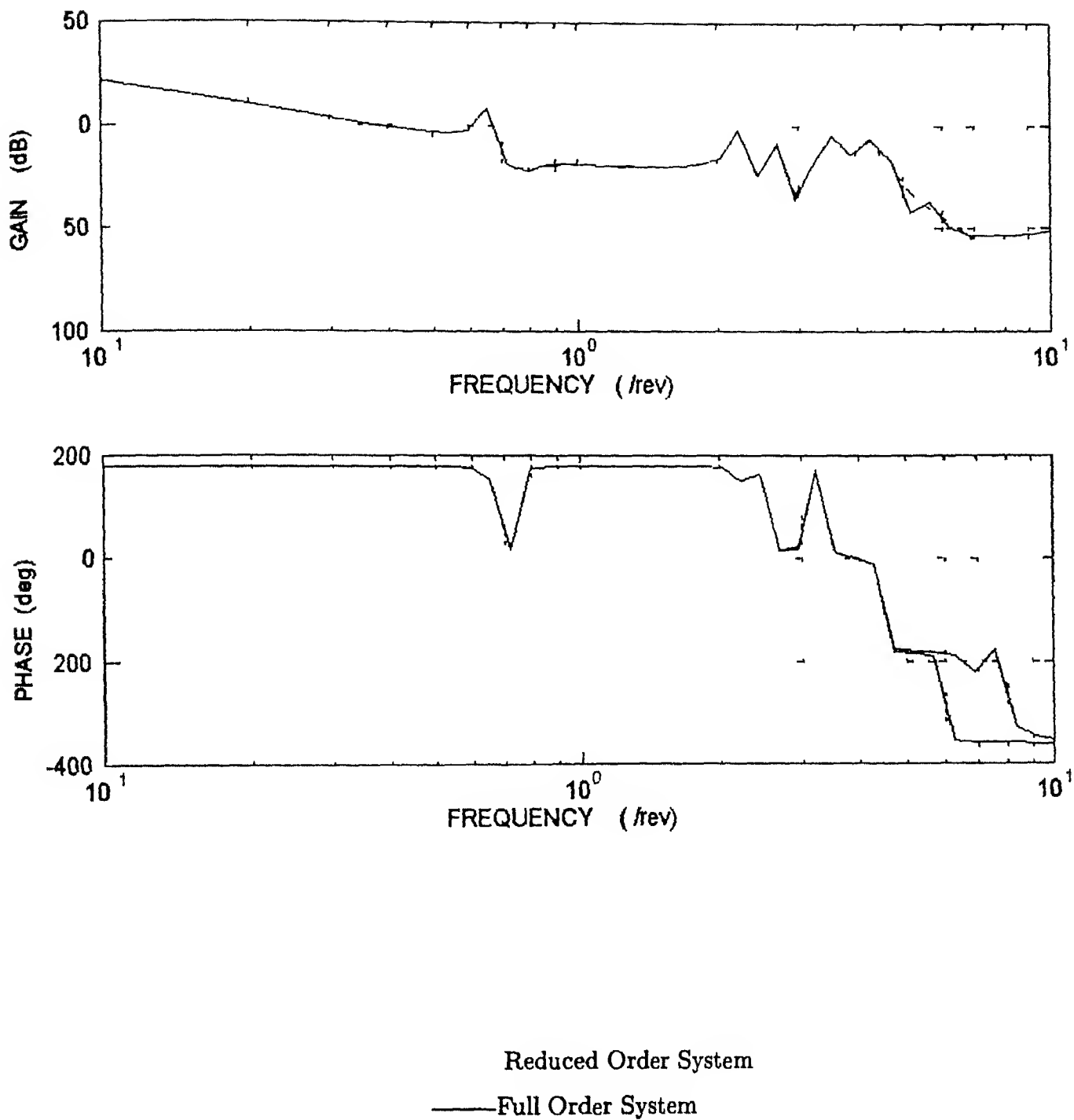


Figure 3 7 Comparison of Frequency Response of the Full and Reduced Order Model (Node No 17)

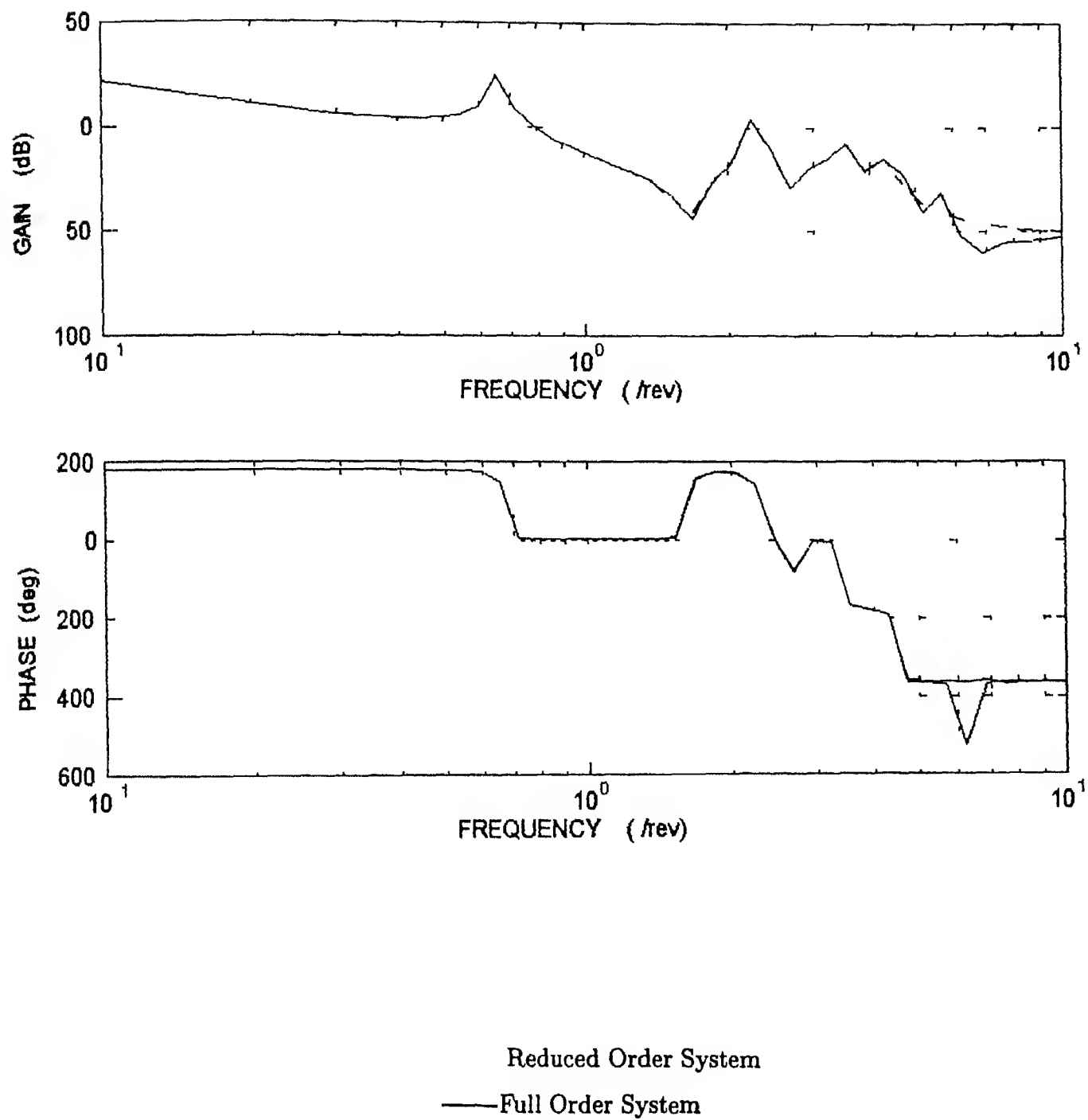


Figure 3 8 Comparison of Frequency Response of the Full and Reduced Order Model (Node No 23)

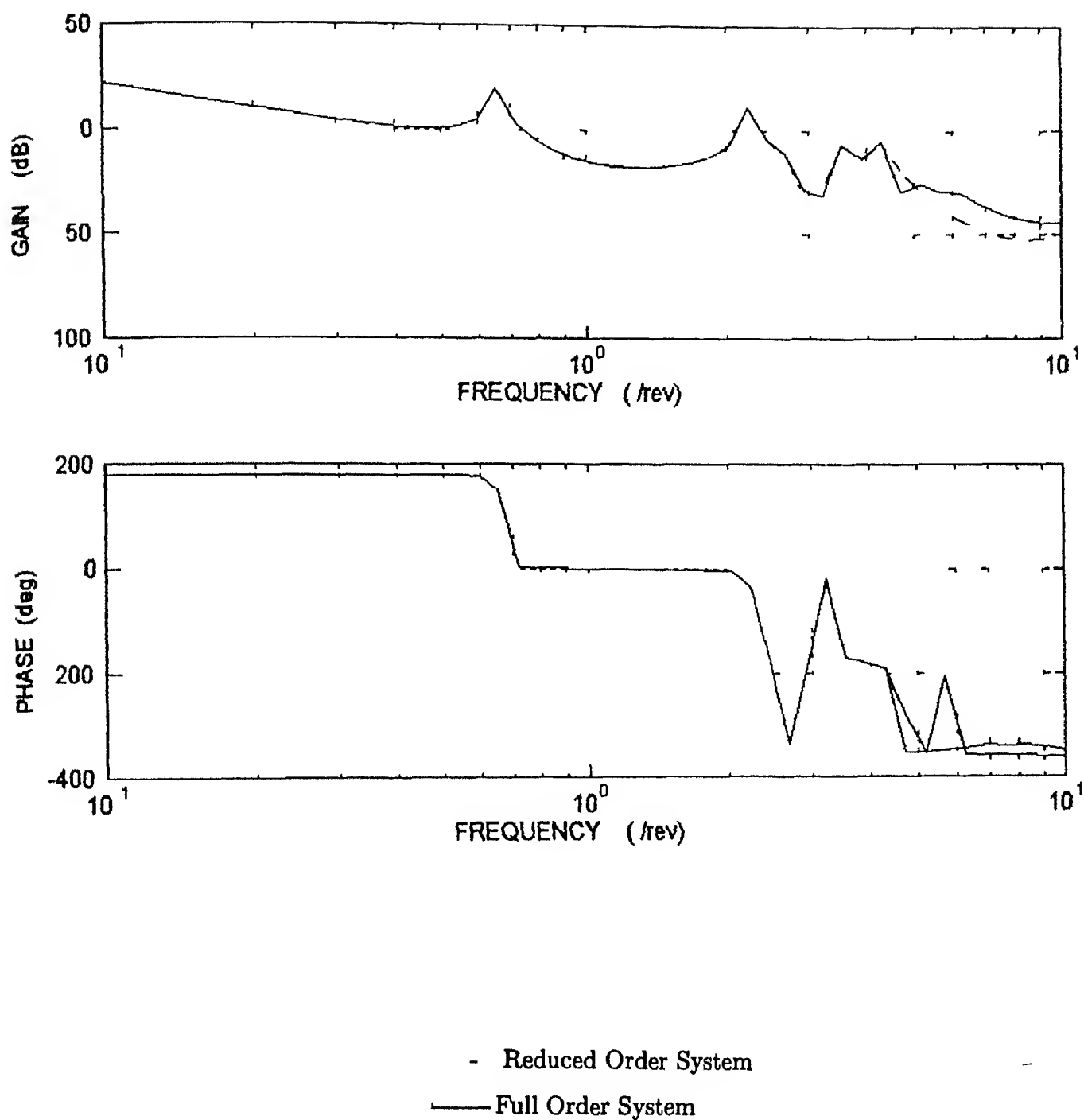
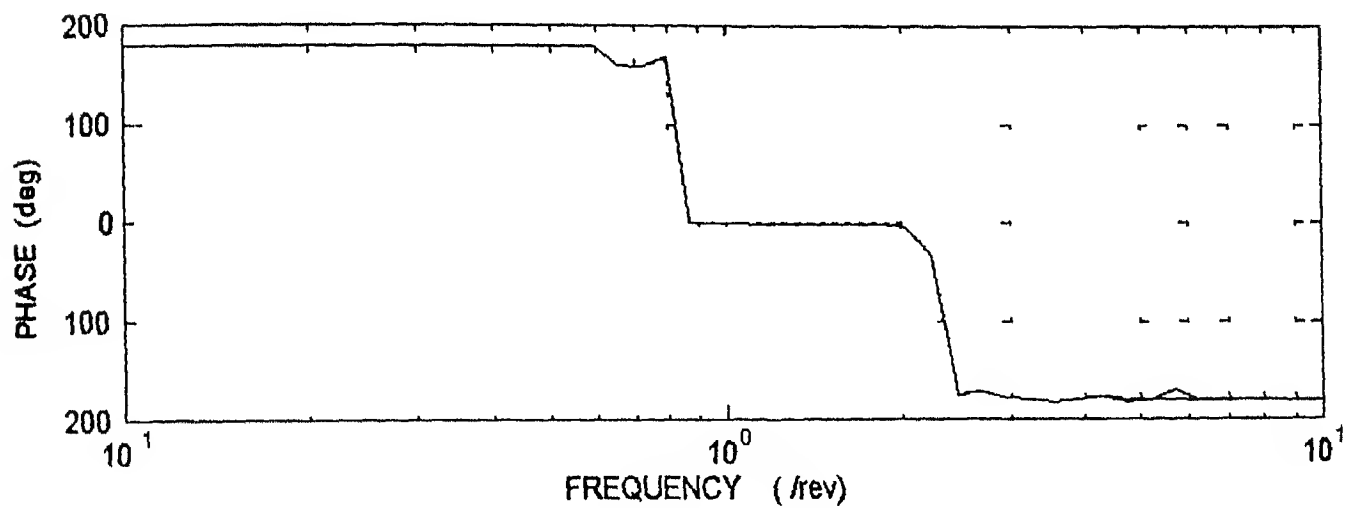
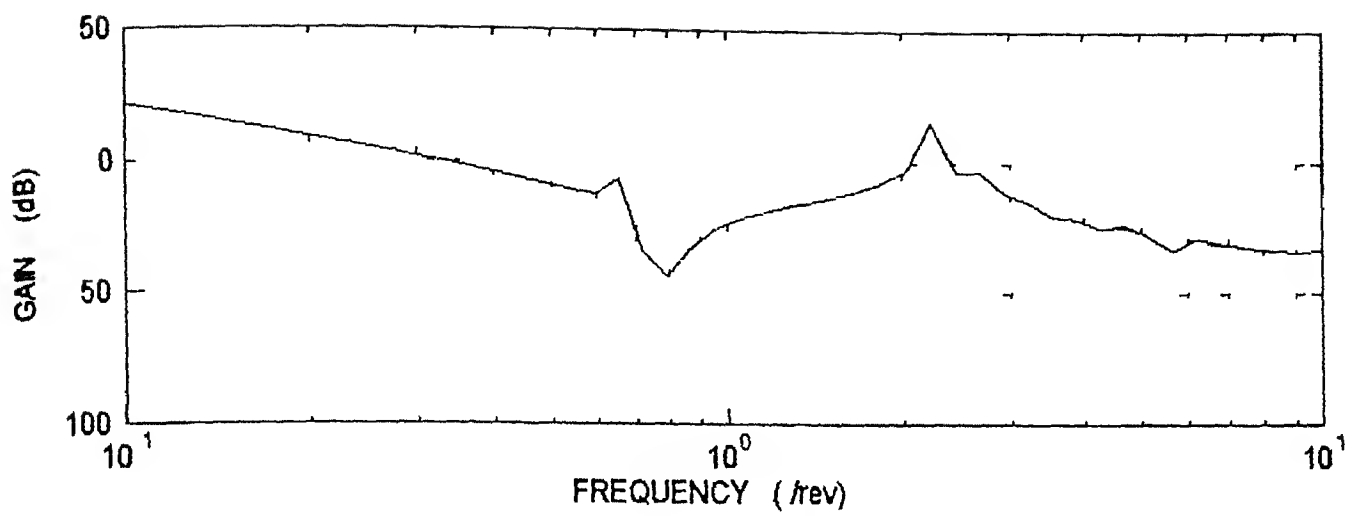


Figure 3 9 Comparison of Frequency Response of the Full and Reduced Order Model (Node No 34)



Reduced Order System  
 — Full Order System

Figure 3 10 Comparison of Frequency Response of the Full and Reduced Order Model (Node No 39)

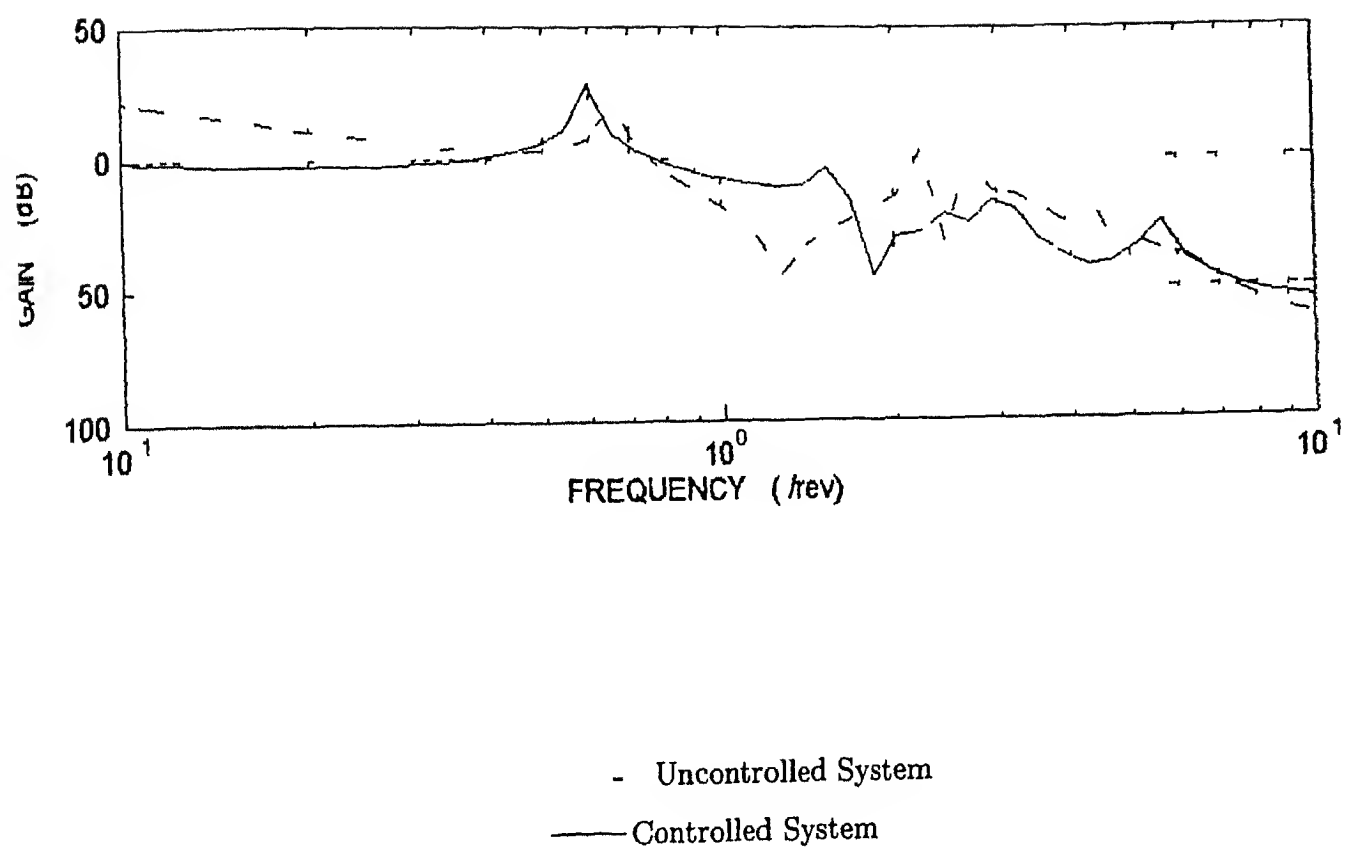
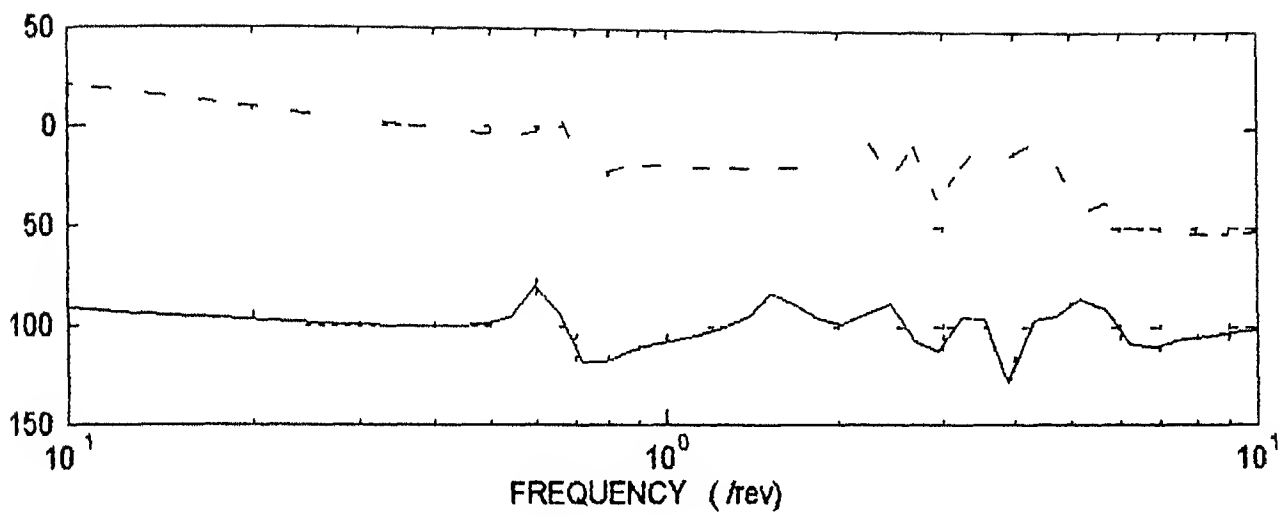


Figure 3 11 Frequency Response of the Uncontrolled and Closed Loop Controlled System (Node No 8)



Uncontrolled System  
— Controlled System

Figure 3 12 Frequency Response of the Uncontrolled and Closed Loop Controlled System (Node No 17)

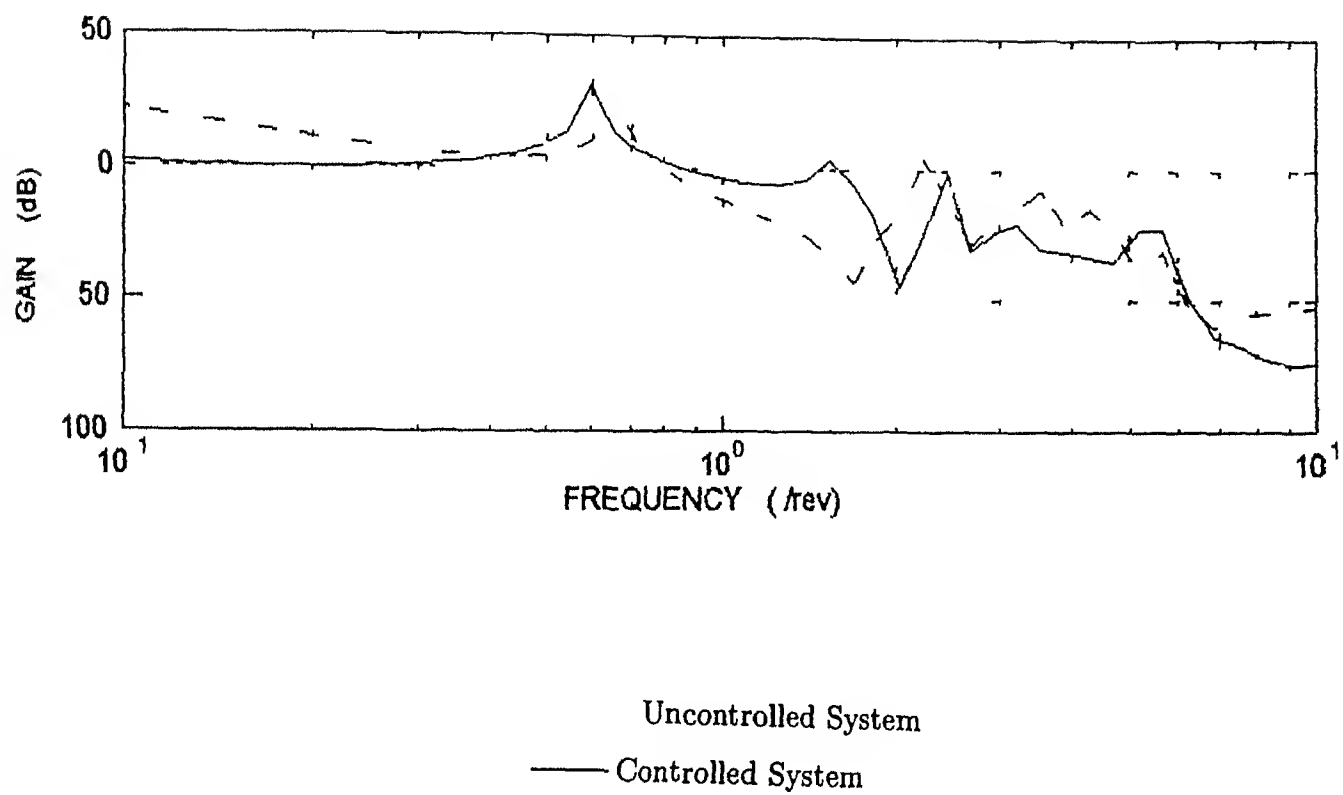
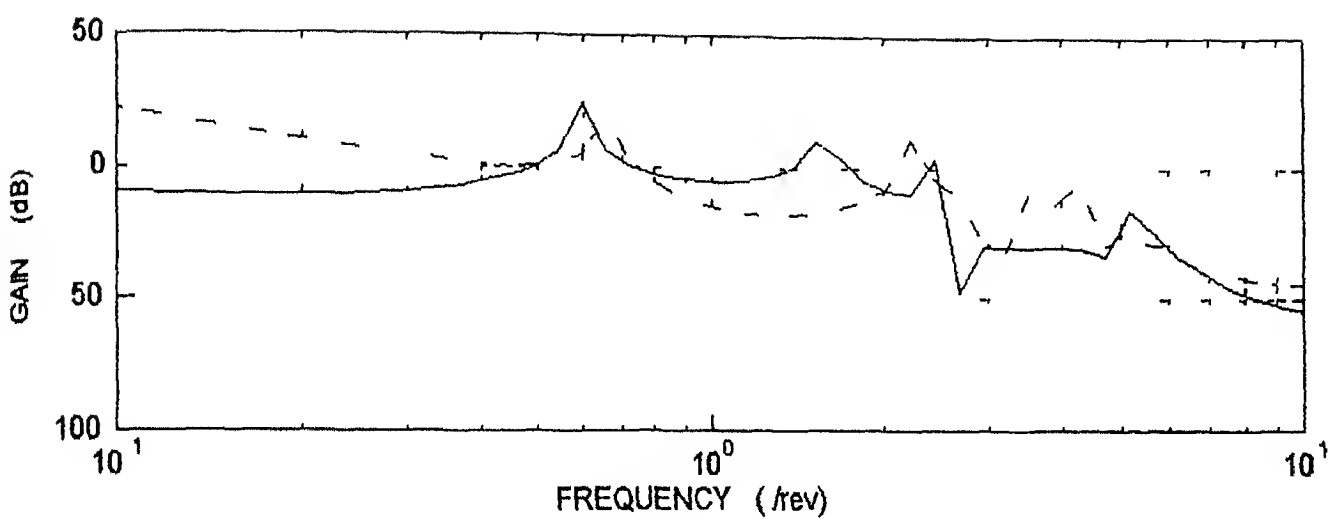


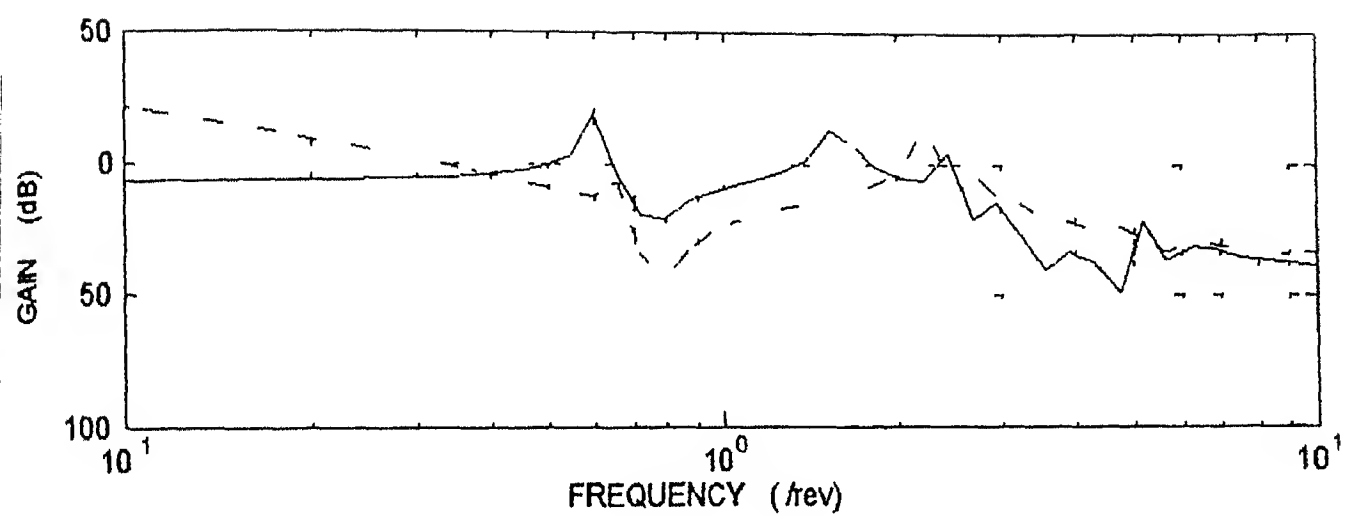
Figure 3 13 Frequency Response of the Uncontrolled and Closed Loop Controlled System (Node No 23)





Uncontrolled System  
 ——— Controlled System

Figure 3 14 Frequency Response of the Uncontrolled and Closed Loop Controlled System (Node No 34)



Uncontrolled System  
 — Controlled System

Figure 3 15 Frequency Response of the Uncontrolled and Closed Loop Controlled System (Node No 39)

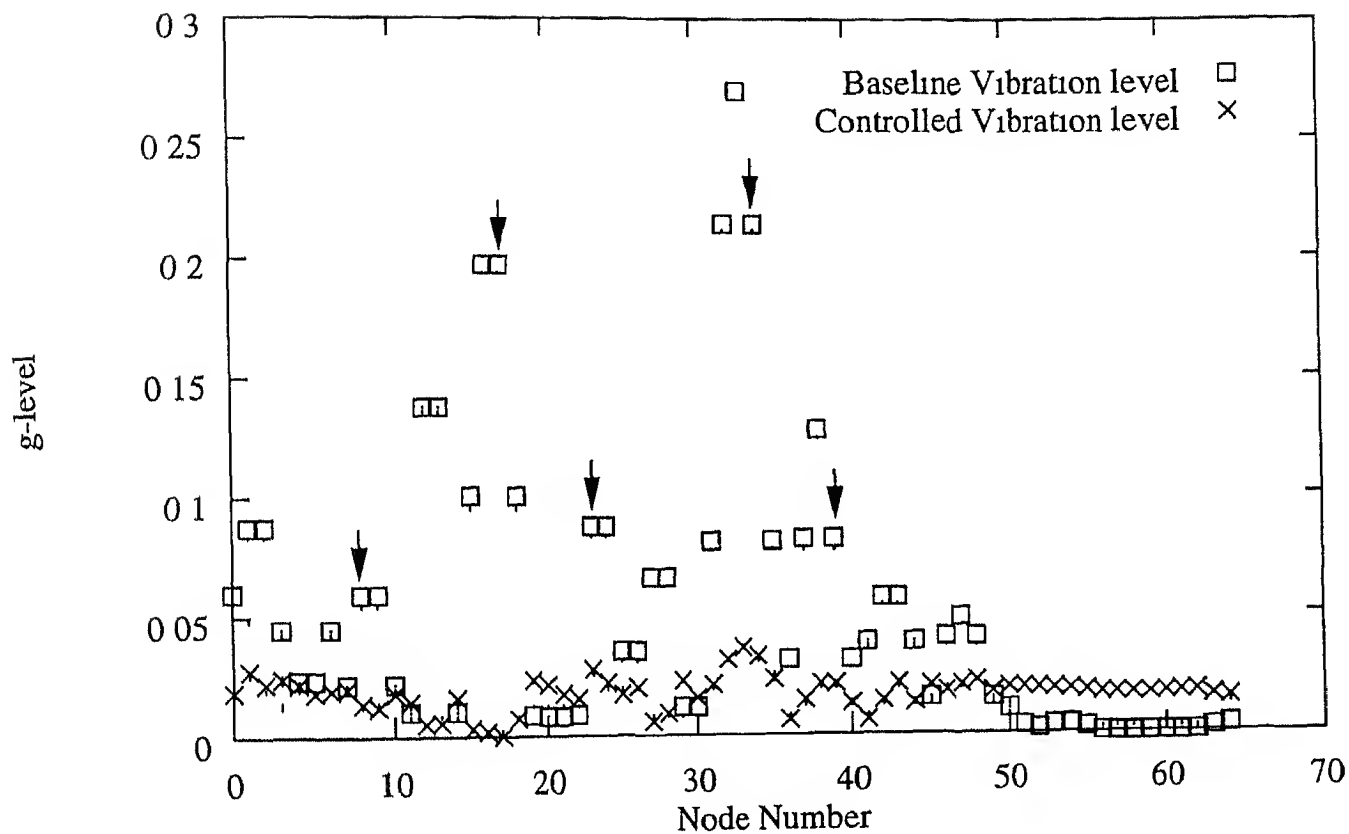


Figure 3 16 Comparison of Baseline and Closed Loop Controlled Vibratory Levels (Node Locations 8, 17, 23, 34, 39)

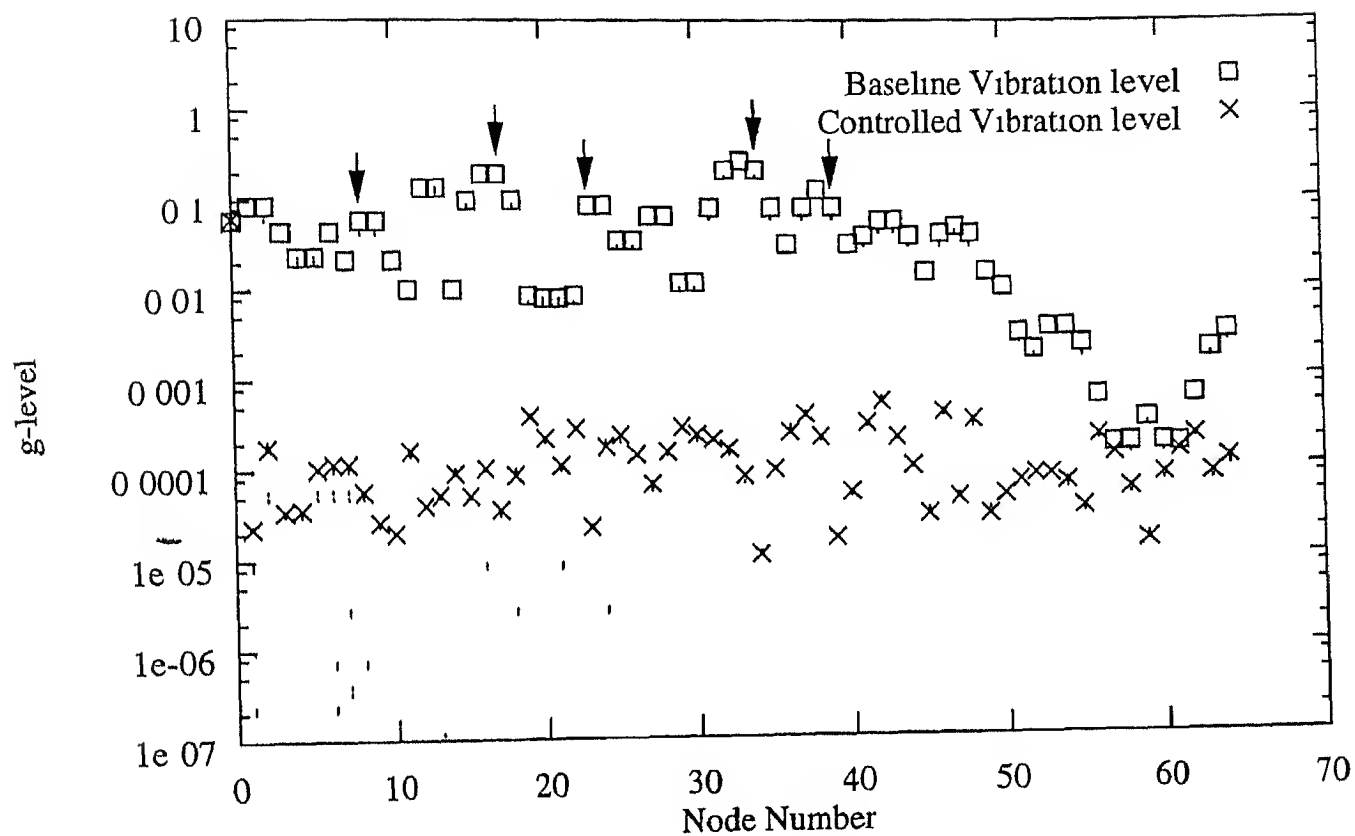


Figure 3 17 Comparison of Baseline and Open Loop Controlled Vibratory Levels (Node Locations 8, 17, 23, 34, 39)

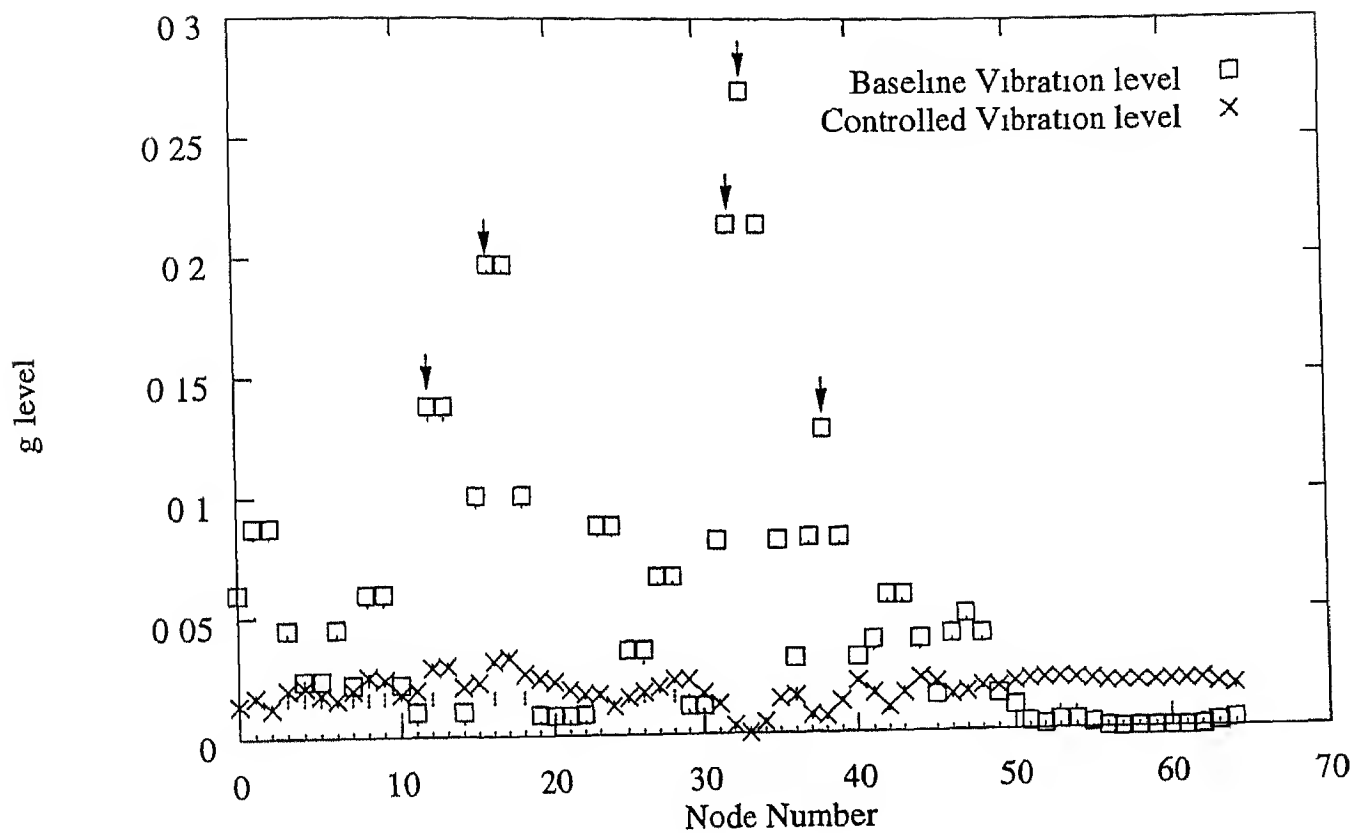


Figure 3 18 Comparison of Baseline and Closed Loop Controlled Vibratory Levels (Node Locations 12, 16, 32, 33, 38)

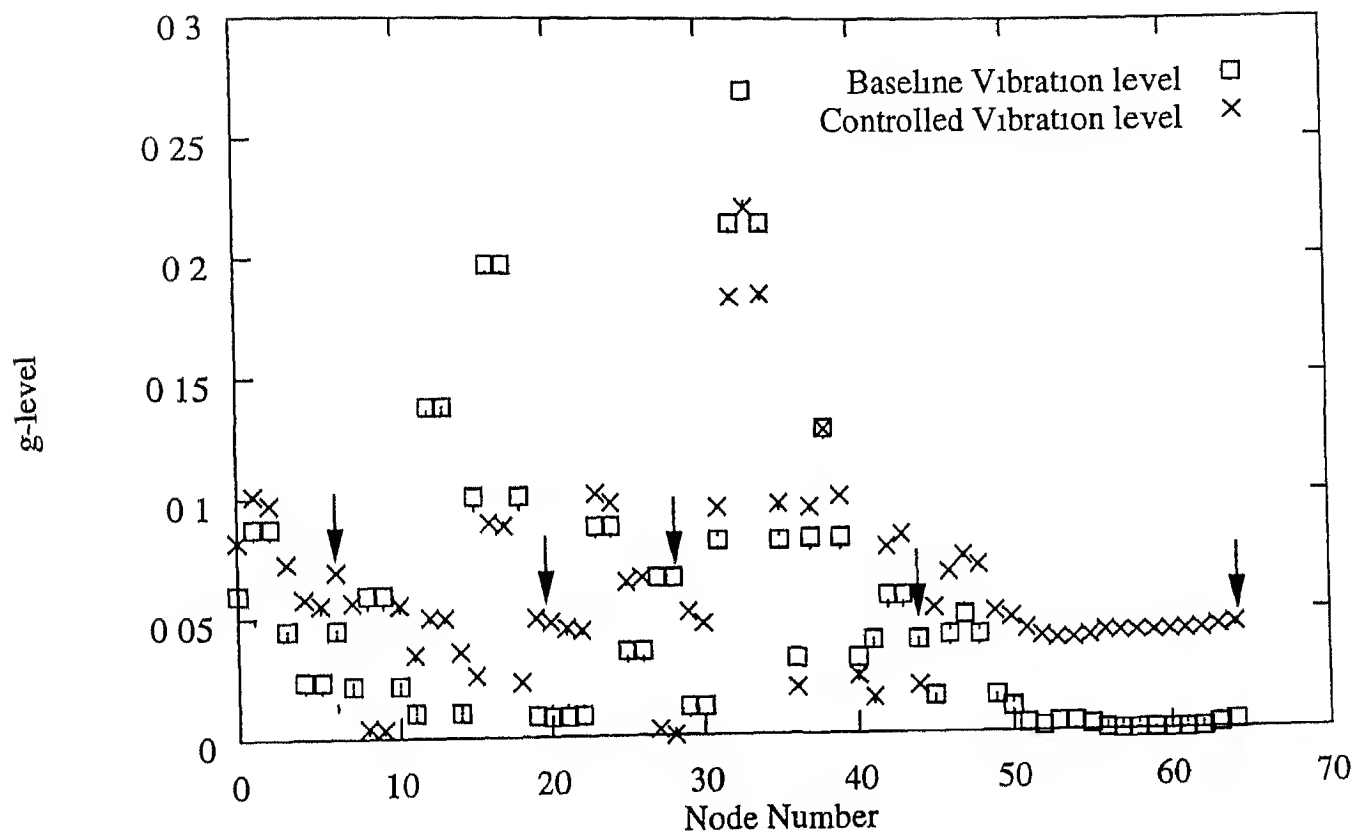


Figure 3 19 Comparison of Baseline and Closed Loop Controlled Vibratory Levels (Node Locations 6, 20, 28, 44, 64)

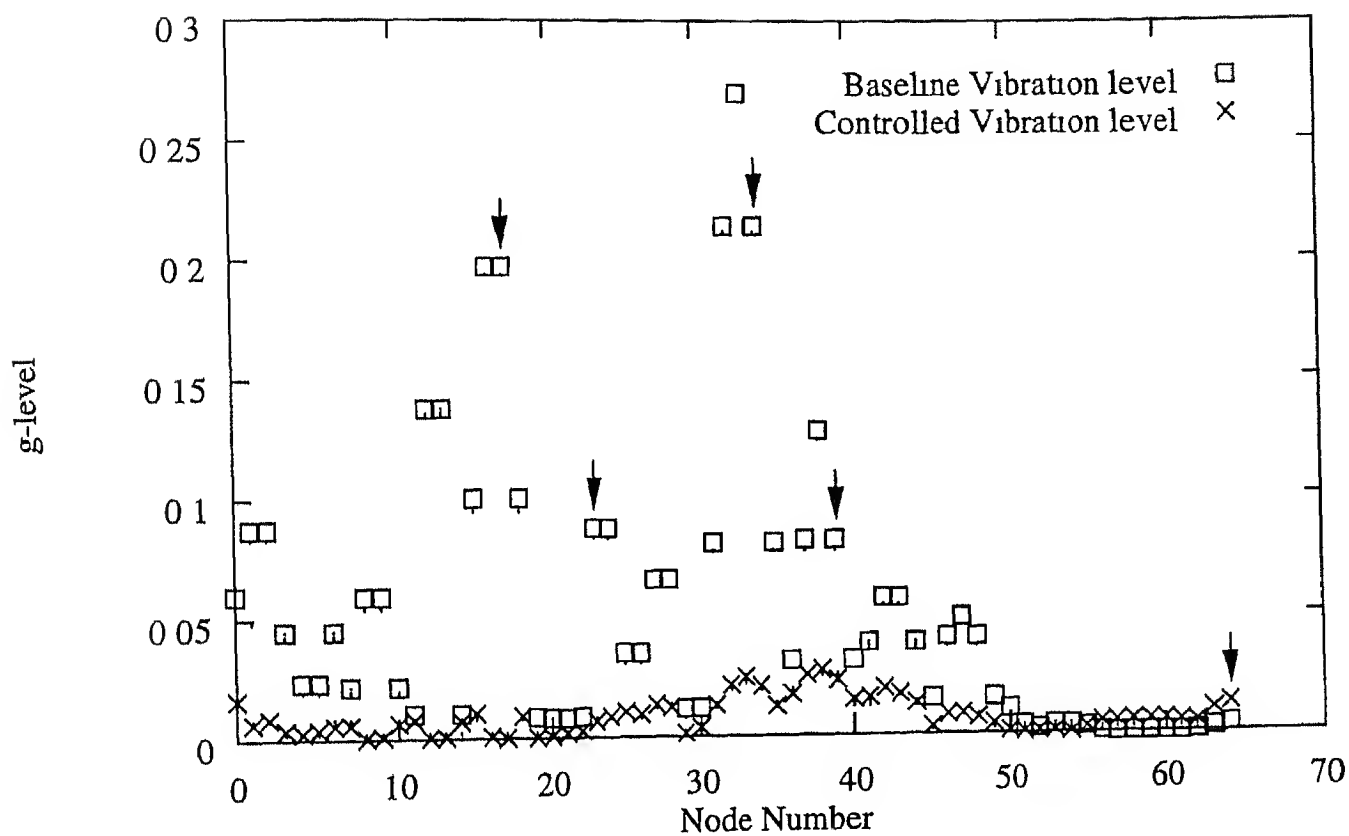


Figure 3 20 Comparison of Baseline and Closed Loop Controlled Vibratory Levels (Node Locations 17, 23, 34, 39, 64)

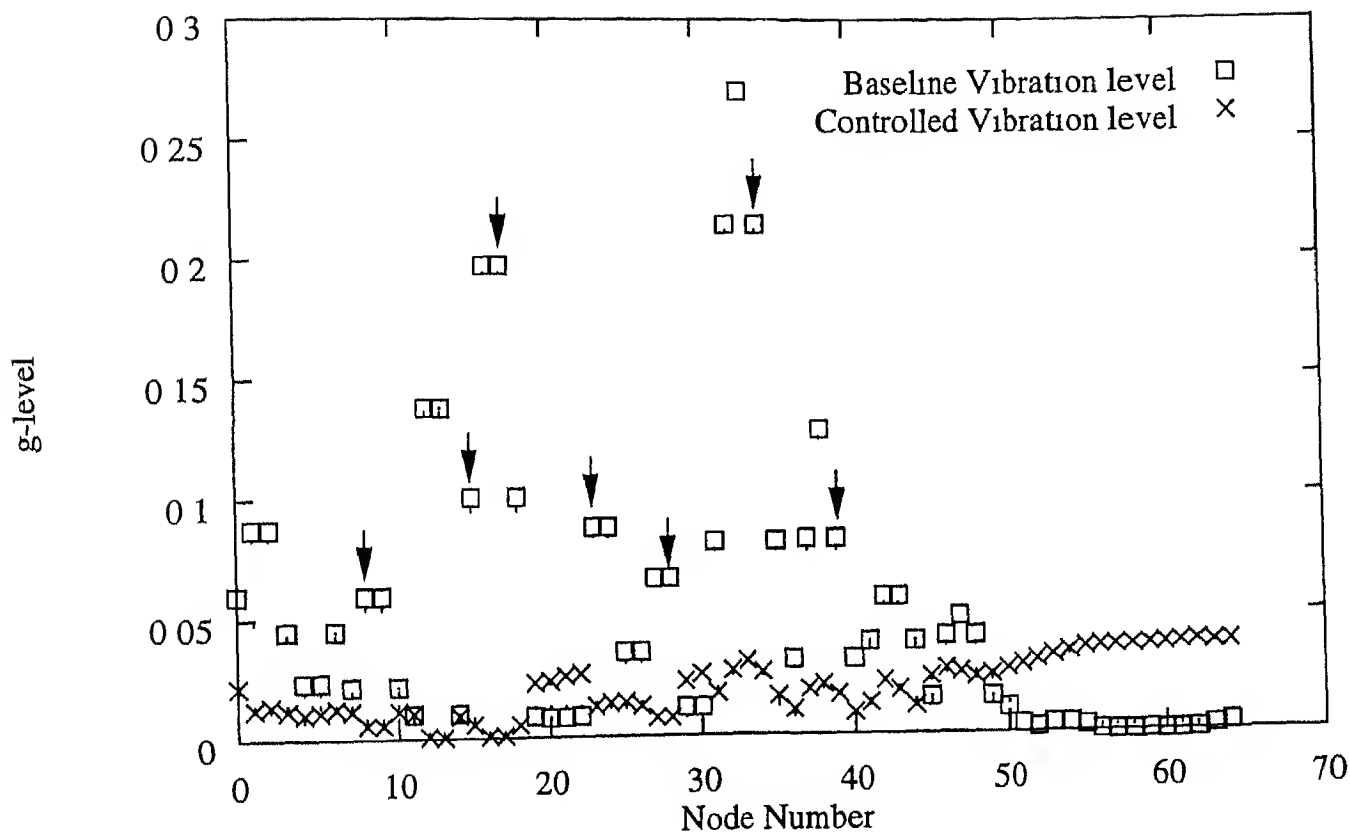


Figure 3.21 Comparison of Baseline and Closed Loop Controlled Vibratory Levels (Node Locations 8, 17, 23, 34, 39, 15, 28)

CENTRAL LIBRARY  
I I T KANPUR

Acc No. A 126846



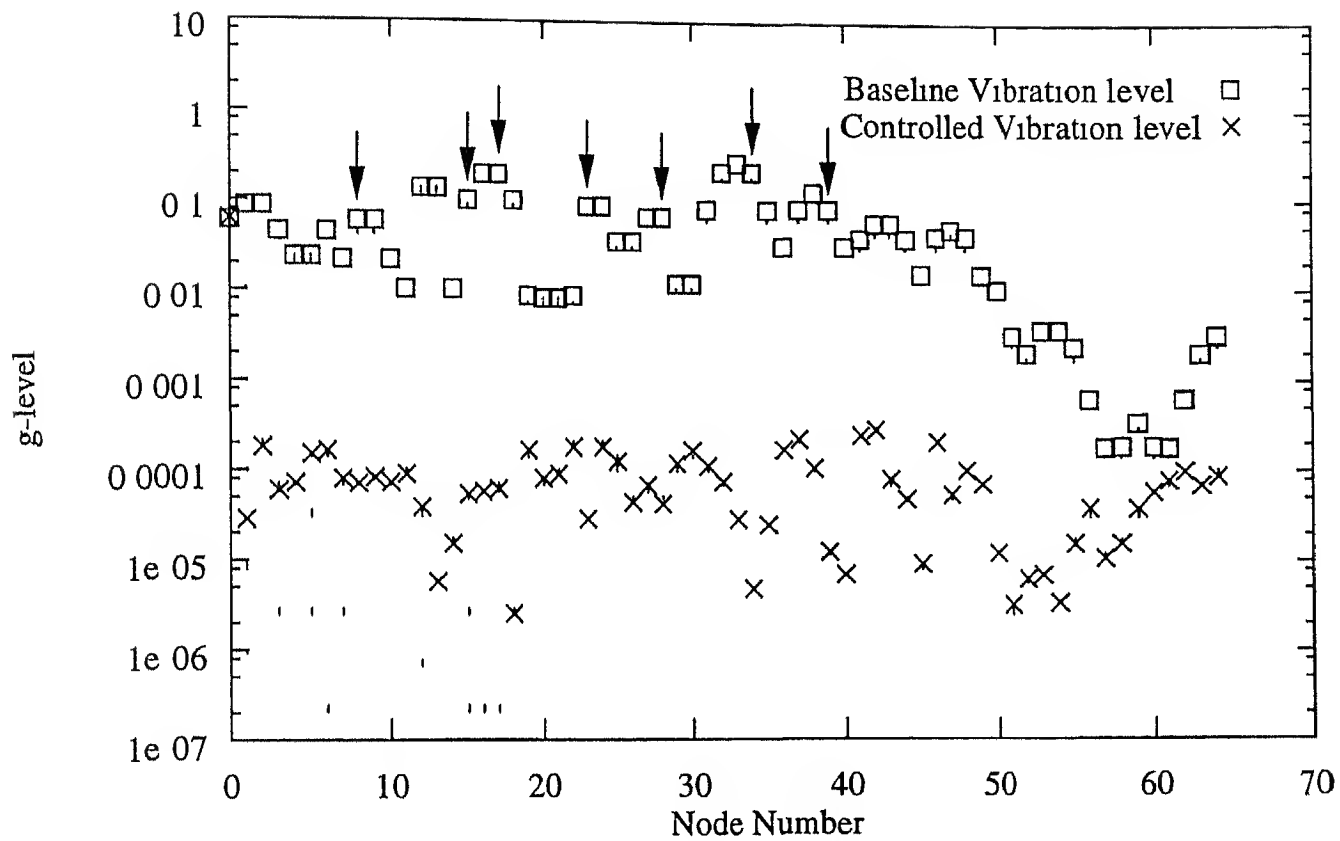


Figure 3 22 Comparison of Baseline and Open Loop Controlled Vibratory Levels (Node Locations 8, 17, 23, 34, 39, 45, 58)

# Chapter 4

## Concluding Remarks

In this thesis, the formulation and design of a closed loop control scheme for vibration minimisation of the helicopter has been carried out. The full order helicopter system(52 order) was decomposed to flexible mode subsystem(46 order) and rigid body mode subsystem(6 order). A reduced order model was found out, that satisfactorily approximated the full system, using the technique of balanced realisation based model order reduction technique. A stabilising controller is designed for the reduced system using factorisation theory and internal model principle for disturbance reduction.

For the choice of five optimal sensor locations, the closed loop control gives reduced vibration levels as compared to the baseline values, in the fuselage and gearbox. In the tail region though, there is observed to be an increase in vibration from the baseline value. This could be because there were no sensors chosen from the tail region. On having a sensor in the tail along with the optimal sensors, the level of vibration in the tail portion is seen to be lowered. In the open loop control formulation, as compared to closed loop design, there is more reduction in vibration, in the fuselage. But in the gearbox, it is observed that there is an increase in vibration after open loop control.

An arbitrary choice of high vibration node locations for sensor placement gave good vibration reduction as compared to arbitrary low vibration sensor locations. Thus, it is observed that sensor locations have a significant influence on the level of vibration reduction in fuselage structure.

It is seen that there is very small variation in the magnitudes and phase angles of the control force, in open loop control scheme, on increasing the number of optimal sensor locations from five to seven. While for closed loop scheme, for seven sensor locations,

the control force is seen to be reduced by a factor of 10 as compared with five sensor locations. The level of vibration reduction is almost similar for five and seven number of optimal sensor locations.

## APPENDIX A

### Parametrization Of All Stabilising Controllers

Using factorisation theory Ref [24] we obtain a doubly coprime stable factorization of a plant transfer matrix  $P$ . Using this, the formula for all stabilising compensators which can also guarantee poles of the closed loop system in a specified region of the complex plane, if required, is obtained

Consider the system transfer matrix  $P$  represented in a state space model as

$$\dot{x} = Ax + Bu$$

$$y = Cx + Du$$

which is denoted in shorthand as

$$P = \begin{pmatrix} A & B \\ C & D \end{pmatrix} = C(sI - A)^{-1}B + D$$

The doubly coprime factorization of  $P$  is defined as follows

**Definition**

A doubly coprime factorization (DCF) of  $P$  over a closed region  $\Omega$  in the complex plane is a factorization of  $P$  as

$$P = ND^{-1} = D^{-1}N$$

such that the following properties are satisfied

- 1  $N, D, \tilde{N}, \tilde{D}$  have no poles in  $\Omega$
- 2 There are transfer matrices  $X, Y, \tilde{X}, \tilde{Y}$  which have no poles in  $\Omega$
- 3  $Y, \tilde{Y}$  are square and nonsingular
- 4  $N, D, \tilde{N}, \tilde{D}, X, Y, \tilde{X}, \tilde{Y}$  satisfy the identity

$$\begin{bmatrix} Y & X \\ -\tilde{N} & \tilde{D} \end{bmatrix} \begin{bmatrix} D & -\tilde{X} \\ N & \tilde{Y} \end{bmatrix} = I$$

The procedure for obtaining  $N, D, \tilde{N}, \tilde{D}$  of a given plant  $P$  from its state space discription is given below Suppose the given system

$$P = \begin{pmatrix} A & B \\ C & D \end{pmatrix}$$

is minimal Select matrices  $K$  and  $H$  such that  $A_K = A - BK$  and  $A_H = A - HC$  have no eigen values in  $\Omega$  Then  $N, D, \tilde{N}, \tilde{D}, X, Y, \tilde{X}, \tilde{Y}$  are given as [24]

$$\tilde{N} = \begin{pmatrix} A_H & B - HD \\ C & D \end{pmatrix}$$

$$\tilde{D} = \begin{pmatrix} A_H & H \\ -C & I \end{pmatrix}$$

$$N = \begin{pmatrix} A_K & B \\ C - DK & D \end{pmatrix}$$

$$D = \begin{pmatrix} A_K & B \\ -K & I \end{pmatrix}$$

$$X = \begin{pmatrix} A_H & H \\ K & 0 \end{pmatrix}$$

$$Y = \begin{pmatrix} A_H & B - HD \\ K & I \end{pmatrix}$$

$$\tilde{X} = \begin{pmatrix} A_K & H \\ K & 0 \end{pmatrix}$$

$$\tilde{Y} = \begin{pmatrix} A_K & H \\ C - DK & I \end{pmatrix}$$

### Formula For All Stabilising Controllers

In the DCF above, if  $\Omega$  is a compliment of an open connected domain  $\Gamma$  in the left half of the complex plane, then the factors  $N, D, \tilde{N}, \tilde{D}, X, Y, \tilde{X}, \tilde{Y}$  are all stable transfer functions with all the poles in  $\Gamma$

The well known formula which makes use of the DCF and expresses all the stablising compensators  $C(s)$  such that the closed loop system with the transfer matrix from  $w$  the disturbance input to  $z$ , the regulated output has all its poles in  $\Gamma$  is given as follows Let

Q be any proper rational transfer matrix with no poles in  $\Omega$  then

$$\begin{aligned} C &= \{ (Y - Q\tilde{N})^{-1}(X + Q\tilde{D}), \det(Y - Q\tilde{N}) \neq 0 \} \\ &= \{ (X + DQ)(Y - NQ)^{-1}, \det(\tilde{Y} - NQ) \neq 0 \} \end{aligned}$$

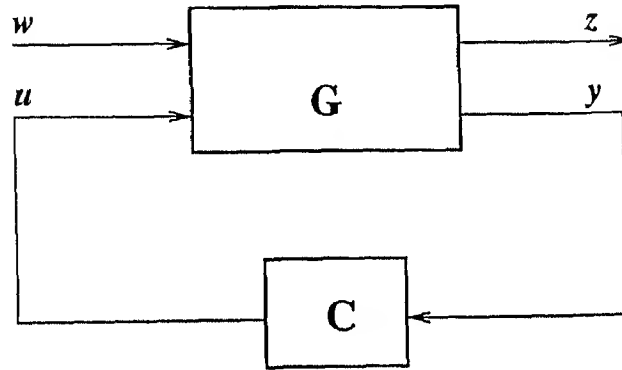
Thus we obtain the parametrization of all compensators that stabilize a given plant P

This parametrization is affine in the free parameter Q

## APPENDIX B

### The Four Block Control Problem

In the standard block diagram used for four block problem, as shown in fig ()  $w$  is the exogeneous input, typically consisting of command signals, disturbances and sensor noises  $u$  is the control signal  $z$  is the output to be controlled, its components typically being tracking errors, filtered actuator signals etc  $y$  is the measured output A feedback controller  $C$  is attached to the plant to form the feedback system



For  $G$ , the generalised plant given by the four block transfer matrix

$$G = \begin{bmatrix} G_{11} & G_{12} \\ G_{21} & G_{22} \end{bmatrix}$$

The equations of the feedback system are then given by

$$z = G_{11}w + G_{12}u$$

$$y = G_{21}w + G_{22}u$$

$$u = -Cy$$

Hence for a well posed system (ie, when  $\det(I+GC) \neq 0$ ), the transfer matrix denoting the response  $z$  due to exogenous input  $w$  is obtained as

$$y = T_{zw}w$$

where

$$T_{zw} = G_{11} - G_{12}C(I + G_{22}C)^{-1}G_{21}$$

*Standard problem –*

The standard problem is to find a real rational proper  $C$  to minimize the  $H_\infty$  norm of  $T_{zw}$ , the transfer matrix from  $w$  to  $z$  under the constraint that  $C$  stabilizes  $G$ . All the requirements like robustness, disturbance rejection, tracking accuracy etc can be captured in the transfer matrix between  $w$  and  $z$ . One such procedure using model matching theory is outlined below

### Model matching Theory

The transfer matrix between  $w$  and  $z$  can be written as [7]

$$T_{zw} = T_1 - T_2QT_3,$$

with  $C(s)$  given in Appendix A.  $T_1$ ,  $T_2$  and  $T_3$  are defined as follows. Let the standard set up of Fig (5.1) in Appendix A has state space realization

$$G(s) = \begin{pmatrix} A & B_1 & B_2 \\ C_1 & D_{11} & D_{12} \\ C_2 & D_{21} & D_{22} \end{pmatrix}$$

Choose  $F$  and  $H$  such that  $A_F = A - BF$  and  $A_H = A - HC$  are stable. Then  $T_1$ ,  $T_2$  and  $T_3$  are given by

$$T_1(s) = \begin{pmatrix} \underline{A} & \underline{B} \\ \underline{C} & D_{11} \end{pmatrix}$$

$$\begin{aligned} \underline{A} &= \begin{bmatrix} A_F & B_2F \\ 0 & A_H \end{bmatrix} \\ \underline{B} &= \begin{bmatrix} B_1 \\ B_1 - HD_{21} \end{bmatrix} \\ \underline{C} &= \begin{bmatrix} C_1 - D_{12}F & D_{12}F \end{bmatrix} \end{aligned}$$



$$T_2(s) = \begin{pmatrix} A_F & B_2 \\ C_1 - D_{12}F & D_{12} \end{pmatrix}$$

$$T_3(s) = \begin{pmatrix} A_H & B_1 - HD_{21} \\ C_2 & D_{21} \end{pmatrix}$$

## APPENDIX C

### Model Reduction Via Balanced Realization

Model reduction is one of the important issues in the dynamic analysis of flexible structures. A model with a large number of degrees of freedom, although useful in a static analysis, can cause numerical difficulties, uncertainties and higher computational costs, if used in dynamical analysis of a system.

For state space models, a methodology for deriving reduced order model is provided in terms of a system's realization in balanced coordinates. The key computational problem there is the calculation of a balancing transformation and the matrices of the balanced realization.

A simple way to decrease the order of a model is to delete everything but the controllable and observable part. The problem is, this part of the model is structurally unstable and that any system is in some sense generically controllable and observable. Therefore, one would like to be able to measure the "degree of controllability and observability" of different subspaces of the state space. The most controllable and observable part could then be used as a low order approximation for the model. Ref[17]

Bruce C Moore in his paper, *Principal Component Analysis in Linear Systems: Controllability, Observability and Model Reduction* explains this point. The controllability and observability grammians are used to define measures of controllability and observability in certain directions of the state space. The grammians are not invariant under coordinate transformations and it is shown that there exists a coordinate systems in which the grammians are equal and diagonal. The corresponding system representation is called *balanced*. A reduced order model can be obtained from the balanced representation by deleting the least controllable and therefore least observable part.

Consider a linear time invariant continuous time system in state space form

$$\dot{x} = Ax + Bu$$

$$y = Cx + Du$$

where  $A$  is  $n \times n$ ,  $B$  is  $n \times r$  and  $C$  is  $m \times n$

The system is assumed to be controllable and observable, which means that the controllability grammians

$$W_r = \int_0^\tau e^{At} B B^T e^{A^T t} dt$$

and the observability grammian

$$W_o = \int_0^\tau e^{A^T t} C^T C e^{At} dt$$

are both nonsingular for any  $\tau > 0$ . The grammians are not invariant under equivalence transformations on the system. There always exists an equivalent system for which the grammians are equal and diagonal, i.e.

$$W_r = W_o = \Lambda$$

Each state variable is, in a sense, equally strongly coupled to the input and the output in a balanced realization and this lies at the root of the usefulness of these realizations, for model approximations.

Let  $\sigma_i$ ,  $i = 1, 2, \dots, n$  be the singular values of the controllability and observability grammians.

Assume that the state variables have been permuted so that  $\sigma_{i+1} \leq \sigma_i$ ,  $i = 1, 2, \dots, n-1$  and that the balanced system is partitioned as

$$\begin{pmatrix} \dot{x}_1 \\ \dot{x}_2 \end{pmatrix} = \begin{pmatrix} A_{11} & A_{12} \\ A_{21} & A_{22} \end{pmatrix} \begin{pmatrix} x_1 \\ x_2 \end{pmatrix} + \begin{pmatrix} B_1 \\ B_2 \end{pmatrix} u$$

$$y = (C_1 \quad C_2) \begin{pmatrix} x_1 \\ x_2 \end{pmatrix} + Du$$

where  $A_{11}$  is  $k \times k$

Let  $u_1$  and  $u_2$  be the  $L_2$  norm functions that drive the state from the origin to

$\begin{pmatrix} x_1^T(\tau) & 0 \end{pmatrix}^T$  and  $\begin{pmatrix} 0 & x_2^T(\tau) \end{pmatrix}^T$ , in the time interval  $[0, \tau]$

It was shown by Moore that

$$\int_0^\tau \frac{\|u_2\|^2 dt}{\|u_1\|^2 dt} \geq \frac{\sigma_k}{\sigma_{k+1}} \frac{\|x_2(\tau)\|^2}{\|x_1(\tau)\|^2}$$

If  $\sigma_k \gg \sigma_{k+1}$  and  $u_1$  and  $u_2$  have the same norms it follows that

$$\|x_2(\tau)\| \ll \|x_1(\tau)\|$$

In the other words, the part  $x_2$  of the state is much less affected by the input than the part  $x_1$

Analogously, let  $y_1$  and  $y_2$  be the zero input responses from  $\begin{pmatrix} x_1^T(\tau) & 0 \end{pmatrix}^T$

and

$$\begin{pmatrix} 0 & x_2^T(\tau) \end{pmatrix}^T$$

Then

$$\int_0^\tau \|y_2(t)\|^2 dt \ll \int_0^\tau \|y_1(t)\|^2 dt$$

if  $\sigma_k \gg \sigma_{k+1}$

and

$$\|x_1(0)\| = \|x_2(0)\|$$

This means that the  $x_2$  part of the state affects the output much less than the  $x_1$  part

Thus we see that the  $x_2$  part of the state does not affect the input-output behaviour of the system very much if

$$\sigma_{k+1} \ll \sigma_k$$

The algorithm to obtain the transformation matrix which gives a balanced realization is given in Sec (2.2.2)

## Algorithm for Model Order Reduction

To obtain an approximate model of the original system a balanced realization of the original system is obtained and then simply truncated by discarding those parts relating to the state variables which are most weakly coupled to the inputs and outputs Ref[13,15]

A workable algorithm that gives a reduced model of order  $k$  after balancing is ,

- Find  $W_c$  and  $W_o$  for the given system  $(A, B, C)$
- Let  $k =$  Order of reduced order model
- Compute cholesky factors of the grammians  $W_r$  and  $W_o$

$$W_r = L_r L_r^T$$

and

$$W_o = L_o L_o^T$$

- Compute singular value decomposition of the product of cholesky factors

$$L_o^T L_r = U \Lambda V^T$$

where  $U$  and  $V$  are unitary matrices and  $\Lambda$ , a diagonal matrix

- Find,  $S = \Lambda^{-1/2}$  and let

$U_1 =$  Matrix containing only the first  $k$  columns of  $U$

$V_1 =$  Matrix containing only the first  $k$  columns of  $V$

- Form the balancing transformations,

$$T_1 = L_o * U_1 * S$$

$$T_2 = L_r * V_1 * S$$

- Then, the reduced model  $(A_k, B_k, C_k, D)$  is,

$$A_k = T_1^T * A * T_2$$

$$B_k = T_1^T * B$$

$$C_k = C * T_2$$

$$D_k = D$$

Thus we obtain a balanced, reduced,  $k$ th order model

# Bibliography

- [1] Balas, M J , *Trends in Large Space Structure Control Theory Fondest Hopes Wildest Dreams*, IEEE Trans Automat Contr , Vol 27, No 3, pp 522 533 1982
- [2] Bong, W , Gonzalez,M , *Control Synthesis for Flexible Space Structures Excited by Persistent Disturbances*, Journal of Guidance, Control, and Dynamics, Vol 15 No 1 pp 73 80, 1992
- [3] Chiu, T , Friedmann,P , *ACSR System for Vibration Suppression in Coupled helicopter Rotor/Flexible Fuselage Model*,37th AIAA/ASME/ASCE/AHS/ASC Structures, Structural Dynamics and Materials Conference, April, 1996, Salt Lake City, Utah
- [4] Crews, S T , *Rotorcraft Vibration Criteria A new perspective* Proceedings of the 43 rd Annual Forum of the American Helicopter Society St Louis, May 1987
- [5] Dosch, J , Leo,D , Inman,D , *Modelling and Control for Vibration Suppression of a flexible active structure* Journal of Guidance, Control, and Dynamics, Vol 18, No 2, pp 340 346, 1995
- [6] Francis, B A , Wonham,W M , *The Internal Model Principle of Control Theory*, Automatica, Vol 12, pp 457 465, 1976
- [7] Francis, B A , *A Course in  $H_\infty$  Control Theory*, Lecture Notes in Control and International Sciences, No 88, Springer Verlag, Berlin, 1986
- [8] Fortuna, L , Nunnari, G , Gallo, A , *Model Order Reduction Techniques with Application in Engineering*, Springer Verlag, 1992

- [9] Friedmann, P P , Milliot, T A , *Vibration Reduction in Rotorcraft using Active Control A Comparison of Various Approaches*, Journal Of Guidance Control, and Dynamics, Vol 18, No 4, pp 664 673, 1995
- [10] Gawronski W , Williams, T , *Model Reduction for Flexible Space structures* Journal of Guidance, Control, and Dynamics, Vol 14, No 1 pp 68-76, 1989
- [11] Glover K , *All Optimal Hankel norm Approximations of Linear Multivariable System and their  $L_{\infty}$  Error Bounds*, International Journal of Control Vol 39, No 6 pp 1115 1131, 1984
- [12] Kailath, T , *Linear Systems* Prentice Hall Inc , 1980
- [13] Lub, A J , Heath, M T , Paige, C C , Ward R C *Computation of System Balancing Transformations and other Applications of Simultaneous Diagonalization Algorithms*, IEEE Trans Automat Contr , vol 32, pp 115 121 1987
- [14] Loewy, R G , *Helicopter Vibrations a Tecnological Perspective*, Journal of The American Helicopter Society, Vol 29, No 4, pp 4 30, 1984
- [15] Maciejowski, J M , *Multivariable Feedback Design*, Addison Wesley Publishing Company, 1989
- [16] Patel, R V , Munro, N , *Multivariable System Theory and Design*, Int Series on Systems and Control, Pergamon, 1982
- [17] Pernebo, L , Silverman, L M , *Model Reduction via Balanced State Space Representations*, IEEE Trans Automat Contr , Vol 27, No 2, pp 382 392, 1982
- [18] Reichert, G , *Helicopter Vibration Control A Survey*, Vertica Vol 5, No 1, pp 1 20 1981
- [19] Reichert, G , Huber, H , *Active Control of Helicopter Vibration*, 4th Workshop on Dynamics and Aeroelastic Stability Modeling of Rotorcraft systems, Nov 1991, University of Maryland, Maryland

- [20] Staple A E *An Evaluation of Active Control of Structural Response as a Means of Reducing Helicopter Vibrations*, 15th European Rotorcraft Forum Amsterdam Netherlands, pp 3 17, Sept , 1989
- [21] Udayshankar, A , *Choice of Sensor Locations and Vibration Control in flexible Helicopter Fuselage*, M Tech Thesis, Dept of Aerospace Engineering ,IIT Kanpur India, 1997 IIT Kanpur 1997
- [22] Vasile Sima *Algorithm for Linear Quadratic Optimisation*, Marcel Dekker Inc Newyork 1996
- [23] Venkatesan, C ,Tiwari, N , Mangalick S , *Formulation of Coupled Rotor Gearbox Fuselage Dynamics for Active Vibration Control Studies*, 5th National Seminar on Aerospace Structures, IIT Bombay, India, 1996
- [24] Vidyasagar, M , *Control System Synthesis A Factorisation Approach*, M I T Press Cambridge, 1985
- [25] Welsh, W A , Von Hardenberg, P C , Von hardenberg, P W Staple, A E *Test and Evaluation of Fuselage Vibration Utilizing Active Control of Structural Response Optimising to ADS 27* , 46th Annual Forum of the American Helicopter Society Washington D C , pp 21 37, 1990
- [26] Wolovich, W A , *Automatic Control Systems Basic Analysis and design*, Harcourt Brace College Publishers, 1994



**A**

**126846**

**A**

**126846**

**Date Slip**

This book is to be returned on the  
date last stamped

--

EE-1998-M Mat - ord



A126846